

Age-related increase of kynurenine enhances miR29b-1-5p to decrease both CXCL12 signaling and the epigenetic enzyme Hdac3 in bone marrow stromal cells

Ahmed M. Elmansi^{a,b}, Khaled A. Hussein^c, Sergio Mas Herrero^d, Sudharsan Periyasamy-Thandavan^e, Alexandra Aguilar-Pérez^{f,g,h}, Galina Kondrikova^{a,b}, Dmitry Kondrikov^{a,b}, Nada H. Eisa^{a,b,i}, Jessica L. Pierce^h, Helen Kaiser^h, Ke-Hong Ding^j, Aisha L. Walker^k, Xue Jiang^l, Wendy B. Bollag^{j,m,n,o,p}, Mohammed Elsalanty^q, Qing Zhong^r, Xing-ming Shi^{m,r}, Yun Su^r, Maribeth Johnson^{r,s}, Monte Hunter^m, Charles Reitman^t, Brian F. Volkman^u, Mark W. Hamrick^{h,m,n}, Carlos M. Isales^{j,m,n,v}, Sadanand Fulzele^{m,n}, Meghan E. McGee-Lawrence^{h,m,n,*}, William D. Hill^{a,b,h,n,o,**}

^a Department of Pathology and Laboratory Medicine, Medical University of South Carolina, Charleston, SC 29403, United States of America

^b Ralph H. Johnson Veterans Affairs Medical Center, Charleston, SC 29403, United States of America

^c Department of Oral Surgery and Medicine, National Research Centre, Cairo, Egypt

^d Dept. of Psychiatry, Universitat de Barcelona, Spain

^e Georgia Cancer Center, Augusta University, Augusta, GA 30912, United States of America

^f Department of Anatomy and Cell Biology, Indiana University School of Medicine in Indianapolis, IN, United States of America

^g Department of Cellular and Molecular Biology, School of Medicine, Universidad Central del Caribe, Bayamon 00956, Puerto Rico

^h Cellular Biology and Anatomy, Medical College of Georgia, Augusta University, Augusta, GA 30912, United States of America

ⁱ Department of Biochemistry, Faculty of Pharmacy, Mansoura University, Mansoura 35516, Egypt

^j Department of Medicine, Medical College of Georgia, Augusta University, Augusta, GA 30912, United States of America

^k Department of Medicine, Vascular Medicine Institute, University of Pittsburgh School of Medicine, Pittsburgh, PA 15261, United States of America

^l Department of Rehabilitation, Shengjing Hospital of China Medical University, Shenyang, Liaoning, China

^m Department of Orthopaedic Surgery, Medical College of Georgia, Augusta University, Augusta, GA 30912, United States of America

ⁿ Center for Healthy Aging, Medical College of Georgia, Augusta University, Augusta, GA, 30912, United States of America

^o Charlie Norwood Veterans Affairs Medical Center, Augusta, GA 30904, United States of America

^p Department of Physiology, Medical College of Georgia, Augusta University, Augusta, GA 30912, United States of America

^q Department of Oral Biology, Dental College of Georgia, Augusta University, Augusta, GA 30912, United States of America

^r Department of Neuroscience and Regenerative Medicine, Medical College of Georgia, Augusta University, Augusta, GA 30912, United States of America

^s Department of Population Health Science, Augusta University, Augusta, GA 30912, United States of America

^t Orthopaedics and Physical Medicine Department, Medical University of South Carolina, Charleston, SC 29403, United States of America

^u Biochemistry Department, Medical College of Wisconsin, Milwaukee, WI 53226, United States of America

^v Division of Endocrinology, Diabetes and Metabolism, Medical College of Georgia, Augusta University, Augusta, GA 30912, United States of America

ARTICLE INFO

Keywords:

Kynurenine
AhR
CXCL12
Hdac3
miR-29b-1-5p

ABSTRACT

Mechanisms leading to age-related reductions in bone formation and subsequent osteoporosis are still incompletely understood. We recently demonstrated that kynurenine (KYN), a tryptophan metabolite, accumulates in serum of aged mice and induces bone loss. Here, we report on novel mechanisms underlying KYN's detrimental effect on bone aging.

We show that KYN is increased with aging in murine bone marrow mesenchymal stem cells (BMSCs). KYN reduces bone formation via modulating levels of CXCL12 and its receptors as well as histone deacetylase 3 (Hdac3). BMSCs responded to KYN by significantly decreasing mRNA expression levels of CXCL12 and its cognate receptors, CXCR4 and ACKR3, as well as downregulating osteogenic gene RUNX2 expression, resulting

* Correspondence to: M.E. McGee-Lawrence, Department of Cellular Biology and Anatomy, Medical College of Georgia, Augusta University, 1460 Laney Walker Blvd., CB1101, Augusta, GA 30912, United States of America.

** Correspondence to: W.D. Hill, Department of Pathology and Laboratory Medicine, Medical University of South Carolina, Thurmond/Gazes Bldg-Room 506A, 30 Courtenay Drive, Charleston, SC 29403, United States of America.

E-mail addresses: mmcgeelawrence@augusta.edu (M.E. McGee-Lawrence), hillwi@musc.edu (W.D. Hill).

<https://doi.org/10.1016/j.bonr.2020.100270>

Received 9 March 2020; Accepted 6 April 2020

Available online 23 April 2020

2352-1872/ © 2020 The Author(s). Published by Elsevier Inc. This is an open access article under the CC BY-NC-ND license

(<http://creativecommons.org/licenses/by-nc-nd/4.0/>).

in a significant inhibition in BMSCs osteogenic differentiation. KYN's effects on these targets occur by increasing regulatory miRNAs that target osteogenesis, specifically miR29b-1-5p.

Thus, KYN significantly upregulated the anti-osteogenic miRNA miR29b-1-5p in BMSCs, mimicking the up-regulation of miR-29b-1-5p in human and murine BMSCs with age. Direct inhibition of miR29b-1-5p by antagomirs rescued CXCL12 protein levels downregulated by KYN, while a miR29b-1-5p mimic further decreased CXCL12 levels. KYN also significantly downregulated mRNA levels of Hdac3, a target of miR-29b-1-5p, as well as its cofactor NCoR1. KYN is a ligand for the aryl hydrocarbon receptor (AhR). We hypothesized that AhR mediates KYN's effects in BMSCs. Indeed, AhR inhibitors (CH-223191 and 3',4'-dimethoxyflavone [DMF]) partially rescued secreted CXCL12 protein levels in BMSCs treated with KYN. Importantly, we found that treatment with CXCL12, or transfection with an miR29b-1-5p antagomir, downregulated the AhR mRNA level, while transfection with miR29b-1-5p mimic significantly upregulated its level. Further, CXCL12 treatment downregulated IDO, an enzyme responsible for generating KYN. Our findings reveal novel molecular pathways involved in KYN's age-associated effects in the bone microenvironment that may be useful translational targets for treating osteoporosis.

1. Introduction

Aging is accompanied by a universal, gradual decline in the integrity and functionality of organs and tissues. While every organism, organ, tissue, or cell population is affected by aging differently, the outcome is universally accompanied by a deterioration in well-being (López-Otín et al., 2013). The skeletal system, which is an active, responsive and dynamic tissue, is no exception (Lee et al., 2017). In fact, aging is the major risk factor for osteoporosis development (Infante and Rodriguez, 2018; Coipeau et al., 2009). The specific mechanisms underlying age-related bone loss remain incompletely defined, but are crucial to understand. Bone is a heterogeneous tissue made up of extracellular matrix (ECM) and different cell populations including mesenchymal stem cells (MSCs), pre-osteoblasts, osteoblasts, osteocytes, bone lining cells, osteoclasts, a complex vasculature system, and the hematopoietic system (Schönherr and Hausser, 2000; Manolagas, 2000; Manolagas and Parfitt, 2010; Schaffler et al., 2013; Matic et al., 2016; Kim et al., 2017). MSCs make up a small percentage of bone cells, but play a vital role in bone modeling and remodeling, fracture repair, and bone aging (da Silva Meirelles, 2006; Granero-Moltó et al., 2009). The balance between osteogenic and adipogenic MSC differentiation in bone marrow is tightly regulated and imperative for bone health (Coipeau et al., 2009; Stenderup, 2003; Tzeng et al., 2018). The literature reports a skewed differentiation pattern of bone marrow mesenchymal stem cells (BMSCs) with age, with both an overall decline in numbers and a shifting from osteogenic to more adipogenic differentiation (Lefterova et al., 2008; Kim and Ko, 2014; Chen et al., 2016). According to Infante et al. (Infante and Rodriguez, 2018), this shift from osteogenesis to adipogenesis in the aging bone marrow MSC population is orchestrated by a number of factors including transcription factors, miRNAs, autophagy levels, cell-extrinsic factors, and epigenetic modifications of DNA.

One such factor of interest is kynurenine (KYN), a primary active metabolite of tryptophan (TRP) that is produced by ROS-mediated oxidation and the action of indoleamine 2,3 dioxygenase-1 or -2 (IDO1 or IDO2) (Metz et al., 2014; Reyes Ocampo et al., 2014; Brooks et al., 2016; Lob et al., 2009; Merlo and Mandik-Nayak, 2016). A high KYN/TRP ratio is correlated with low bone mineral density (BMD) (Apalset et al., 2014). The essential amino acid TRP is crucial for anabolic BMSCs pathways, including those supporting cell proliferation and differentiation, but KYN inhibits these pathways (El Refaey et al., 2015). KYN is thought to mainly act through the aryl hydrocarbon receptor (AhR) (Mezrich et al., 2010; Kurz et al., 2011). Once activated, cytoplasmic AhR is transported into the nucleus where it binds the aryl hydrocarbon receptor nuclear translocator (ARNT) and acts as a transcription factor for a wide array of genes (Murray et al., 2014; Beischlag et al., 2008). We recently tested the hypothesis that a high KYN/TRP ratio mimics the aged bone environment and leads to decreased bone mass in mice, showing that a low TRP/high KYN diet leads to significant bone loss and high marrow adiposity in mice, resembling an

aged bone phenotype (Hamrick et al., 2006; Refaey et al., 2017). We also recently reported elevated KYN concentrations in the bone marrow of aged humans (Kim et al., 2019).

KYN's negative effects on the skeletal system may be mediated by cytokine and epigenetic factors that impact BMSCs. Stromal cell-derived factor 1 (SDF-1 or CXCL12) (Carbone et al., 2017; Herberg et al., 2013; Mortensen and Hill, 2015) is implicated in myriad stem cells functions including cellular proliferation, differentiation, migration, and homing to niche sites (Cheng et al., 2017; Bromage et al., 2014; Yang et al., 2018a; Li et al., 2007; Broxmeyer et al., 2005). CXCL12 has multiple splice variants, the most common of which are CXCL12 α and CXCL12 β (Yu et al., 2006). Both isoforms act mainly through CXCR4 and CXCR7 (i.e., atypical chemokine receptor 3 [ACKR3]) receptors to achieve various downstream effects (Reid et al., 2018; Quinn et al., 2018; Sanchez-Martin et al., 2012). We previously reported that CXCL12 levels decline in bone marrow interstitial fluid with aging, while increasing in the peripheral circulation, which correlates with deteriorating bone health in older subjects (Carbone et al., 2017; Periyasamy-Thandavan et al., 2018). Our group and others have reported that CXCL12 is important for osteogenic differentiation primarily by augmenting the pro-osteogenic effects of BMP-2. CXCR4 signaling is required for the activation of the BMP-2R and increases BMP-2 mediated osteogenesis (Yang et al., 2018a; Herberg et al., 2014a; Herberg et al., 2015). Additionally, targeted deletion of CXCL12 BMSCs results in reduced trabecular bone content and increased bone marrow adiposity (Tzeng et al., 2018). Regarding epigenetic factors, histone deacetylases (Hdacs) are integrally involved in bone homeostasis. Hdacs remove acetyl groups from lysine residues in histones, which changes chromatin structure and in turn affects gene expression altering many signal transduction pathways. Histone deacetylase 3 (Hdac3) is expressed in osteoblasts and plays a critical role in bone development by binding to the osteogenic transcription factor Runx2 to regulate osteoblastic gene expression (Bradley et al., 2011). Conditional deletion of Hdac3 in osteoprogenitor cells (Hdac3-CKO) causes a reduction in osteoblastic activity and produces a low bone mass phenotype with increased BM adipogenesis (Trivedi et al., 2007). Another epigenetic factor that influences BMSC behavior is microRNAs (miRNAs) via effects on cell cycle, apoptosis, proliferation, stem cell maintenance, and differentiation (Khordadmehr et al., 2019; Cheng et al., 2005; Goldar et al., 2015) (Farina et al., 2014) (Wang et al., 2010; Skog et al., 2008; Valadi et al., 2007). MiRNAs are ~20 nucleotide RNAs that bind to mRNAs and post-transcriptionally regulate gene expression of the targeted mRNAs. Pre-miRNAs are processed to generate two partially complementary strands, the normally active guide strand and the passenger strand that is typically degraded and inactive. Several miRNAs play an important role in controlling osteogenic and osteoclastogenic differentiation in the bone marrow, making them valuable new diagnostic biomarkers for bone health (Kureel et al., 2014; Vimalraj et al., 2014; Lee et al., 2013). We have identified one of these as the passenger strand of the key osteogenic microRNA-29b-1 (miR-

29b-1-5p). This novel passenger strand increases with age in human and murine BMSCs (Hill et al., 2016; Periyasamy-Thandavan et al., 2013; Baglio et al., 2013; Lee et al., 2016; Suh et al., 2013a; Shi et al., 2016; Li et al., 2009; William and Hill, 2016). The guide strand (miR-29b-1-3p) has been extensively documented to be critical in different stages of bone formation and fracture healing (Lee et al., 2016; Li et al., 2009; Suh et al., 2013b). Of interest miR-29b-1-3p (and other miR-29 family guide strands) target and suppress the CXCL12 regulator dipeptidyl peptidase-4 (DPP4) (Shi et al., 2016). Therefore, this miRNA is predicted to be central to local bone marrow DPP4 activity and CXCL12 ligand and proteolytic isoform levels. Current studies on miR-29b have focused on the guide strand miR-29b-1-3p (previously miR-29b-1-1) (Li et al., 2009). In contrast, the passenger strand miR-29b-1-5p (previously miR-29b-1-1*) has largely been considered to be a non-functional byproduct of the miR biogenesis process. However, our group has found miR-29b-1-5p to accumulate with aging in human and murine BMSCs (Betel et al., 2010). Further, when it is expressed in BMSCs it can induce aging-like actions targeting osteogenic genes like the CXCL12 axis, and based on in silico analysis, also Hdac3 (Betel et al., 2010).

In this paper, we describe three inter-related mechanisms (CXCL12, Hdac3, miR-29b-1-5p) through which KYN affects BMSCs in aging. These pathways are interconnected, and the crosstalk between them appears to be complex and highly regulated. It also appears that KYN's effect on CXCL12, miR-29b-1, and Hdac3 are all mediated through binding and nuclear translocation of the xenogeneic AhR.

2. Materials and methods

2.1. Animals

C57BL/6J mice were either provided by the National Institute on Aging (Bethesda, MD, USA) aged rodent colony or purchased from Jackson Laboratories (Bar Harbor, ME, USA). Animals were maintained at Augusta University in the Division of Laboratory Animal Services Facility. All aspects of the animal research were conducted in accordance with the guidelines set by Augusta University Institutional Animal Care and Use Committee (AU-IACUC) under AU-IACUC approved Animal Use Protocols. Mice were maintained on a standard 12-h light – 12 h dark protocol and permitted water and food ad libitum.

2.2. Isolation and culture of murine BMSCs

Murine BMSCs were derived from 3, 6, 11, 18, and 27-month-old male C57BL/6J mice at the Augusta University Stem Cell Core Facility. The BMSC isolation process, as well as the MSC characterization and multi-lineage potential (osteogenic, adipogenic and myogenic) have been described previously (Herberg et al., 2013; Zhang et al., 2008). In brief, six to eight mice of each age were euthanized by CO₂ overdose followed by thoracotomy. Whole bone marrow aspirates were flushed from femora and tibiae and BMSCs isolated by negative immunodepletion using magnetic microbeads conjugated to anti-mouse CD11b (#558013) and CD45R/B220 (#551513) (BD Biosciences Pharmingen, San Diego, CA, USA), CD11c, and plasmacytoid dendritic cell antigen (PDCA)-1 (#130-092-283 Miltenyi Biotec, Auburn, CA) followed by positive immunoselection using anti-stem cell antigen (Sca)-1 microbeads (#130-092-529 Miltenyi Biotec, Auburn, CA), according to the manufacturer's recommendations. The enriched single-age pooled BMSC populations were maintained in Dulbecco's Modified Eagle Medium (#10-014-CM DMEM; Cellgro, Mediatech, Manassas, VA, USA) supplemented with 10% heat-inactivated fetal bovine serum (FBS) (#S11150 Atlanta Biologicals, Lawrenceville, GA, USA) and used at 60–70% confluency.

To measure mRNA levels of some markers without culturing or plastic adherence, directly isolated BMSCs were derived from young adult (6–8 months) and geriatric (22–24 month-old) female C57BL/6J mice. Long bones (i.e., humeri, femora, tibiae) were dissected from

mice and placed into mBMSC medium consisting of alpha MEM (#41061 Gibco), 20% FBS, 1% antibiotic/antimycotic, and 1% non-essential amino acids [NEAA] (#11140050 Gibco), on ice. BMSCs were then extracted by flushing marrow and filtering through 70 µm cell strainers.

2.3. Isolation and culture of human BMSCs

A direct-isolation procedure was used to rapidly capture human BMSCs directly from bone. Bone marrow aspirates from the proximal tibia (knee replacement surgery), proximal femur (hip replacement surgery) or iliac crest (spinal fusion surgery) were collected as orthopaedic surgical waste under IRB approval in EDTA blood collection tubes. The bone marrow aspirates were then run over a Ficoll gradient to collect the buffy coat within 30 min of collection. CD271 positive (+) hMSCs were then isolated from the nucleated cell layer using CD271 MicroBead Kits (#130-092-283 Miltenyi Biotec, Auburn, CA) according to the manufacturer's protocol to obtain a highly enriched BMSC population within 2 h of bone marrow aspiration. The cells were counted and frozen, or cultured for 1–2 passages prior to cryopreservation for in vitro cell culture studies. The isolated cells were first confirmed by FACS analysis to be positive for CD73, CD90 and CD105 and negative for CD34, CD45 and CD11b. Corresponding isotype control antibodies were used when cells were sorted according to criteria set by the International Society for Cellular Therapy (ISCT) to define hMSCs (Cao et al., 2015).

Isolating CD271+ cells allows for the direct isolation of BMSCs from orthopaedic patient's bone marrow aspirates within 2 h of collection. This is in contrast to the standard BMSCs isolation process that includes 1–2 day plastic adhesion followed by negative and positive selection and an additional 2–3 week passaging. This is now a standard rapid MSCs isolation method that both reduces the complexity of isolation and maintains cell expression profiles as close to in vivo as possible (Kuçi et al., 2019; Álvarez-Viejo, 2015; Cuthbert et al., 2015; Cox et al., 2012; Poloni et al., 2009).

The isolated cells were tested for multilineage properties, i.e., their capacities for osteogenic, adipogenic and chondrogenic differentiation and the expression levels of key genes (qRT-PCR analysis) regulating these differentiation pathways, including Runx2, Osx and ALP (osteogenic), PPAR γ , and C/EBP β and - α (adipogenic), and Sox-9, type I and type II collagen (chondrogenic). Colony-forming unit-fibroblast (CFU-f) assays were performed to calculate the population doubling capacity. CD271+ MSCs were isolated directly from bone marrow aspirates, washed with standard culture medium composed of DMEM medium (#10-014-CM Corning), 1% antibiotics antimycotics (#15240-062 AA; Invitrogen) and 15% FBS, with low glucose (1 g/l), transferred to 100 mm culture dish and incubated at 37 °C in a humidified atmosphere in 5% carbon dioxide (CO₂). After 24 h, the medium with non-adherent cells is removed, and the adherent cells were carefully washed in DPBS (Dulbecco's phosphate-buffered saline) (#SH30028 HyClone) and further expanded in fresh culture medium. Culture-expanded CD271+ MSCs of passage 1–2 were used for in vitro studies.

2.4. KYN preparation and doses

Human and murine BMSCs were treated with different doses (10, 50, and 200 µM) of L-kynurenine (#K8625 Sigma-Aldrich). Different KYN doses were freshly prepared before administration. Previous data from the literature shows endogenously present KYN levels in the culture media of different cell types is highly variable, ranging from 5 to 60 µM and typically increases with time in culture (Opitz et al., 2011; Yamamoto et al., 2019). Indeed, utilizing an ELISA kit (#E4629 Biovision, Milpitas, CA) we identified that commercial DMEM media (#10-014-CM Corning) itself contains approximately 3–5 µM of KYN (unpublished data). Other researchers have consistently reported various specific dose-dependent effects using wide ranges of KYN doses

(10–300 μM) (Kawasaki et al., 2014; Xiang et al., 2019). Moreover, a recently published paper reported that different doses of KYN (30–500 μM) significantly increased migration in 95D lung cancer cells (Duan et al., 2019). Taking all these different caveats in consideration, we wanted our data to represent three levels of Kyn: 10 μM (low dose close to that of cell-free media and serum levels), 50 μM (medium dose close to the previously reported conditioned media levels secreted by various cell types in culture), and 200 μM (high dose that exceeds the previously reported in vitro levels, falls within the range of KYN doses previously used in literature, and is similar to the in vivo dose used in our previous Kyn studies (Refaey et al., 2017).

2.5. Osteogenic differentiation assay

The ability of culture-expanded MSCs to differentiate into the osteogenic lineage was validated according to earlier described methods (Herberg et al., 2013; Gregory et al., 2004). In brief, cells were plated in 12-well plates at 50000 cells/cm² and cultured in DMEM for 24 h. Culture medium was then aspirated and replaced with StemXVivo Osteogenic/Adipogenic Base Media (#CCM007 R&D Systems) supplemented with StemXVivo Human Osteogenic Supplement (#CCM008 R&D Systems). Treatment-containing medium was replaced 2 times per week. The early osteogenic differentiation marker, Alkaline Phosphatase, was assessed in cell culture media after 7 days using an Alkaline Phosphatase Assay Kit (#ab83369 Abcam). After 3 weeks, osteogenic differentiation was assessed by staining with Alizarin-Red Staining Solution; (#TMS-008-C Millipore Sigma). The cells were fixed with 10% formalin for 20 min at room temperature (RT) and stained with Alizarin-Red Staining Solution for 20 min at RT. Stained monolayers were visualized by phase-contrast microscopy using an inverted microscope (Nikon, Melville, NY). Differentiation was quantified as previously described (Ripoll and Bunnell, 2009). In brief, cells were destained using 10% cetylpyridinium chloride (#855561 Sigma-Aldrich) and collected samples analyzed using a microplate reader at 570 nm.

2.6. Cell density assay

To determine whether KYN affected BMSCs density, we utilized a Crystal violet Assay Kit (#ab232855 Abcam) according to the manufacturer's protocol. In brief, BMSCs were plated in 96 well plates at 5000 cells/well and cultured in DMEM for 24 h. Culture medium was then aspirated and replaced with StemXVivo Osteogenic/Adipogenic Base Media (#CCM007 R&D Systems) supplemented with StemXVivo Human Osteogenic Supplement (#CCM008 R&D Systems) with or without different doses of KYN (10, 50, 200 μM). After 3 days, the culture media was removed and the cells were washed and stained with the Crystal Violet Staining solution for 20 min at RT. Then, the staining solution was removed and the remaining stain was solubilized for 20 min with the Solubilization Solution. Finally, the Crystal Violet stain was quantified using a microplate reader at 595 nm.

2.7. Western blotting

Whole cell lysates of BMSCs were prepared in RIPA lysis and extraction buffer (#89901 ThermoFisher Scientific) containing protease and phosphatase inhibitor cocktail (Millipore Sigma). Protein concentration was determined using Pierce BCA Protein Assay Kit (#23225 ThermoFisher Scientific) and equal amounts (30 μg) of protein lysates were subjected to SDS-PAGE using gradient 4–12% NuPAGE Bis-Tris gels (#NP0321 Invitrogen) and transferred to 0.2 mm nitrocellulose membranes using Power Blotter Select Transfer Stacks (#PB3310 ThermoFisher Scientific).

Membranes were blocked with 5% Bovine Serum Albumin (#A2153 Sigma-Aldrich) in TBST. Osteogenic and Histone deacetylation markers were detected using specific primary antibodies (Table 1). Bound antibodies were visualized with Pierce ECL detection system (#32106

ThermoFisher Scientific) on Amersham Imager 600 (GE Healthcare, Pittsburgh, PA). The intensity of immunoreactive bands was quantified using Image Lab (Bio-Rad, Hercules, CA).

2.8. Quantitative real time polymerase chain reaction (qRT-PCR)

The levels of 18S, CXCL12, CXCR4, ACKR3, IDO-1 and AhR mRNA in human cells undergoing various treatments were assessed using quantitative real-time PCR and TaqMan reagents. Total RNA was isolated from BMSCs and then purified using the RNAeasy kit (#74106 Qiagen, SantaClarita, CA). Purified total RNA was reverse transcribed with High-Capacity cDNA Kits (#4368814 USA – Applied Biosystems). PCR reactions were performed using TaqMan Fast Advanced Master Mix (#4444556 USA – Applied Biosystems). The pre-formulated assay primers used in this study were individual gene-expression assays (#A25576 Applied Biosystems) (Table 2). 18S was used as the endogenous control for mRNA. The target gene was normalized using the endogenous control to calculate $\Delta\Delta\text{Ct}$ values. For real-time PCR, 2 μL of the cDNA sample (100 ng/reaction), 10 μL TaqMan Fast Advanced Master Mix, and 1 μL primer assay were mixed with 7 μL nuclease-free water. All PCR reactions were performed in duplicate.

Gapdh, Hdac3, Hsd11b1, NcoR1, and RUNX2 mRNA levels were assessed using quantitative real-time PCR and SYBR Green reagents. Mouse cells cultured in 6-well plates for 7 days were lysed using TRIzol reagent (#15596-018 Invitrogen), and total RNA was extracted using protocols as previously described. Purified mRNA extracts were reverse transcribed (RT; Bio-Rad C1000 Thermal Cycler, California, USA) to cDNA using commercially available SuperScript III First-Strand Synthesis RT reagents (#11752-050 Invitrogen). Gene expression was determined by real-time semi-quantitative PCR analysis (qPCR; Bio-Rad CFX Connect PCR System, California, USA) using 37.5 ng of cDNA per 15 μL well volume with QuantaBio PerfeCTa SYBR Green Supermix (#95054-500 VWR) and SYBR Green gene specific primers (Table 3). Gene expression levels were quantified using the comparative threshold cycle ($2^{-\Delta\Delta\text{Ct}}$) method. Transcript levels were normalized to the reference gene Gapdh.

Murine miR-29b-1-5p and miR-29b-1-3p levels were assayed using the TaqMan reagents mentioned above and the results were normalized to U6 snRNA (USA – Applied Biosystems). For human miRNA analysis, the expression levels of miR-29b-1-5p and miR-29b-1-3p were measured by miScript qPCR and were normalized to RNU-6 expression (Qiagen, SantaClarita, CA). The catalog numbers for different TaqMan and SYBR green primers are listed in Tables 2 and 3, respectively.

2.9. KYN enzyme linked Immunosorbent assay (ELISA)

Murine bone marrow derived mesenchymal stem cells (BMSCs) of 6 and 18 month old were seeded separately in 6-well flat bottom plates (100,000 cells/well). The cells were grown in DMEM media supplemented with 10% fetal bovine serum and 1 \times of Antibiotic/Antimycotic Solution (#15240062 Invitrogen) at 37 °C, 5% CO₂ incubator. After 24 h and 48 h of incubation, a media sample was collected from each cell line, centrifuged for 20 min at 1000 \times g at 4 °C, transferred to new tube and stored in –80 °C until used. Kynurenine (KYN) ELISA Kit (#E4629 Biovision, Milpitas, CA) was used to measure kynurenine concentration in media samples by following the manufacturer's

Table 1
Specific antibodies used for WB protein analysis.

Protein	Antibody company	Catalog no.
β -Actin	Sigma-Aldrich	A2228
Hdac3	Abcam	Ab7030
H4	Cell Signaling	2935P
Acetyl-H4	Cell Signaling	8647P
Runx2	Abcam	ab76956

Table 2
TaqMan mRNA and miRNA pre-formulated gene specific primer assay IDs.

Gene	Assay ID/cat. no.
18S	Mm03928990
CXCL12	Mm00445553_m1
CXCR4	Mm1996749
ACKR3	Mm02619632_s1
IDO-1	Mm00492590_m1
AhR	Mm00478932_m1
miR-29b-1-5p	Mmu-482721_mir
miR-29b-1-3p	Mmu481300_mir
U6 snRNA	Cat. no. 4427975
Hs-RNU6	Cat. no. MS00033740

Table 3
SYBR Green mRNA gene specific primer sequences.

Gene	Forward sequence	Reverse sequence
Gapdh	GGGAAGCCATCACCATCTT	GCCTCACCCATTGTGATGT
Hdac3	GCATTGAGGACATGGGGAA	TTTCGGACAGTGTAGCCACC
Hsd11b1	ACTCAGACCTCGCTGTCTCT	TGGGTCATTTTCCCAGCCAA
NcoR1	TTATCGGAGCCACTACCCA	CAGGTAAGCAGCAGCAGGAT
RUNX2	GGCACAGACAGAAGCTTGATGA	GAATGCGCCTAAATCACTGA

instructions.

2.10. CXCL12 α enzyme linked Immunosorbent assay (ELISA)

CXCL12 α was measured as described previously (Carbone et al., 2017; Herberg et al., 2013). Briefly, the CXCL12 capture antibody (R&D Systems, Minneapolis, MN) was incubated in sodium bicarbonate buffer overnight. Plates were blocked for 2 h with 1% bovine serum albumin (BSA) in PBS next day. Murine CXCL12 α standards and samples were incubated for 2 h before incubating with the biotinylated anti-CXCL12 α detection antibody (#MAB350 R&D Systems). Streptavidin-horseradish peroxidase (HRP) (#DY998 R&D Systems) was incubated for 20 min followed by the substrate reagent (#DY999 R&D Systems) for 20 min. 2N sulfuric acid was added to stop the enzymatic color reaction and absorbance was read at 450 nm. CXCL12 α protein expression was calculated using standard curves and normalized to total protein, which was quantified using the Pierce BCA Protein Assay Kit. For age-related CXCL12 plasma and bone marrow interstitial fluid levels one set of male C57BL/6 mice from six different age groups (3, 6, 12, 18, 24, and 29 months of age), 10 mice per age group, were obtained from the aged rodent colony at the National Institute on Aging. Our sample is therefore a cross-sectional as opposed to a longitudinal one. Mice were housed individually and all were fed ad libitum on NIH31 diet. Blood was collected via cardiac puncture once mice were euthanized, as per the IACUC protocol, in EDTA tubes which were centrifuged as previously described to obtain plasma, and stored frozen at -80°C . Humeri and tibiae were collected to isolate bone marrow interstitial fluid via flushing of the bone marrow space as previously described (Herberg et al., 2013; Herberg et al., 2014b; Ding et al., 2007).

2.11. Mimic and inhibitor miRNA transfection and AhR inhibition

BMSCs were transfected with either a mimic or inhibitor (antagomir) for miR-29b-1-5p (Cat #YM00471910 and #YI04101505 Qiagen, SantaClarita, CA) according to the manufacturer's protocol. The recommended controls for miR-29b-1-5p mimic and inhibitor were used (Cat #YM00479902 and Cat #YI00199006). In brief, cells were seeded at 25,000–30,000 cells/well in a 24-well plate in 500 μl of an appropriate culture medium containing 10% serum and no antibiotics. For 1–3 h until transfection, cells were incubated under normal growth conditions (typically 37°C and 5% CO_2). miRNA mimics or inhibitors were

resuspended prior to transfection in RNase-free water to achieve the recommended concentration of 20 μM . The miRNA inhibitor and mimic were diluted in Opti-MEM media to give a final miRNA inhibitor concentration of 100 nM and final miRNA mimic concentration of 1 nM for normal transfection experiments and 5 nM for 3'-UTR luciferase assays. HiPerFect transfection reagent (#301705 Qiagen, SantaClarita, CA) was added to the diluted miRNA mimic/inhibitor and mixed by vortexing. Then, the samples were incubated for 5–10 min at room temperature ($15\text{--}25^{\circ}\text{C}$) to allow the formation of transfection complexes. The complexes were added drop-wise onto the cells. BMSCs were incubated with the transfection complexes under their normal growth conditions for 6 h, and then the transfection media was removed and replaced with serum-free media containing the desired treatment. Cell culture media samples were collected for analysis, and cells were lysed and mRNA collected at the end of the incubation period. Negative control miR inhibitor was used as a negative control for miR-29b-1-5p inhibitor, and AllStars Hs Cell Death Control siRNA was used as a negative control for miR-29b-1-5p mimic. For AhR inhibition, AhR antagonist, CH-223191 (#C8124 Sigma-Aldrich) was dissolved in DMSO to make a 2 mg/mL stock solution, and a final concentration of 2 $\mu\text{g}/\text{mL}$ was added to BMSCs culture medium (Asai et al., 2018; Yang et al., 2018b). A second AhR antagonist, 3',4'-dimethoxyflavone (DMF) (#D6571 Sigma-Aldrich), was also used (10 μM).

2.12. Luciferase assay

Culture-expanded human BMSCs were co-transfected with a either wild type or mutated miTarget miRNA 3'-UTR luciferase functional reporter plasmid for CXCL12 or Hdac3 (#HmiT088617-MT06 and #HmiT115117-MT06 GeneCopeia, Rockville, MD) and either miR-29b-1-5p mimic or mimic control (#YM00471910 and #YM00479902 Qiagen, SantaClarita, CA) using Lipofectamine 3000 reagent (#L3000015 ThermoFisher Scientific, Waltham, MA). Mutated plasmids for CXCL12 (at 3 predicted target sites) and Hdac3 (at one predicted target site) were custom made and purchased from GeneCopeia (Rockville, MD). The predicted binding sites for miR-29b-1-5p were determined using the prediction software and database MiRanda (Betel et al., 2010). Dual luciferase activity of the CXCL12 and Hdac3 reporter plasmids were measured 24 h after transfection using Luc-Pair™ Duo-Luciferase High Sensitivity Assay Kit (#LF004 GeneCopeia, Rockville, MD) according to the manufacturer's protocol, and compared to non-targeting miR-transfected controls. The Duo-Luciferase HS Assay Kit was used because it eliminates the need for separate controls to determine if differences are due to differential vector uptake and to normalize the outcomes, e.g. the use of beta-galactosidase which is typically used for normalization to luciferase counts. This is done by including Firefly luciferase (FLuc) and Renilla luciferase (RLuc), where the RLuc signal is used as a control for how much construct was taken into the cell while FLuc signal is used for measuring transcriptional activation. The final signal is expressed as FLuc to RLuc ration to compensate for different transfection efficiencies.

2.13. Statistical analysis

Experiments were performed at least three independent times. Data are expressed as means \pm SD unless stated otherwise. Data were analyzed using GraphPad Prism 7.0 software (GraphPad Software Inc., La Jolla, CA, USA). Student *t*-test was used for comparisons between two groups and analysis of variance (ANOVA) followed by Tukey's multiple comparison test was used for comparisons between 3 or more groups. Null hypotheses were rejected at the 0.05 level. Statistical significance was determined and shown in figures and figure legends.

3. Results

3.1. CXCL12 axis is downregulated with both aging and KYN treatment in murine and human BMSCs

We previously showed that CXCL12 is essential in BMSC osteogenesis (Herberg et al., 2013; Herberg et al., 2015). We also established that KYN contributes to skeletal aging mechanisms and affects the balance between osteogenic and adipogenic differentiation in BMSCs (Refaey et al., 2017). For our initial experiment, we compared the effects of both aging and KYN on the CXCL12 axis. First, we utilized an established ELISA to measure CXCL12 protein levels in murine samples from bone marrow interstitial fluid and plasma at different ages of C57BL/6J mice ($n = 10$ per group). Levels of CXCL12 significantly declined with aging in bone marrow interstitial fluid starting around

12 months of age, while significantly rising in the peripheral circulation after that same age (Figs. 1A, B). The rise in plasma CXCL12 was similar to what we previously observed in human plasma (Carbone et al., 2017), while the decrease in CXCL12 levels in BM interstitial fluid in aged subjects was similar to our previous BM results in mice (Periyasamy-Thandavan et al., 2018). Interestingly, in our in vitro system, BMSCs isolated from 18 months old mice showed significantly increased levels of KYN in their cell culture media compared to BMSCs isolated from 6 months old mice after 48 h of incubation (Fig. 1C).

We also assessed how mRNA expression of CXCL12 and its main receptor, CXCR4, changed in BMSCs with aging. We used BMSCs isolated from mice at the ages of 6, 11, and 27 months. These ages correspond to adult (6 months), adult near the peak accumulation of bone mass prior to bone loss (11 months), which is prior to significant changes in CXCL12 protein levels in the BM interstitial fluid, and

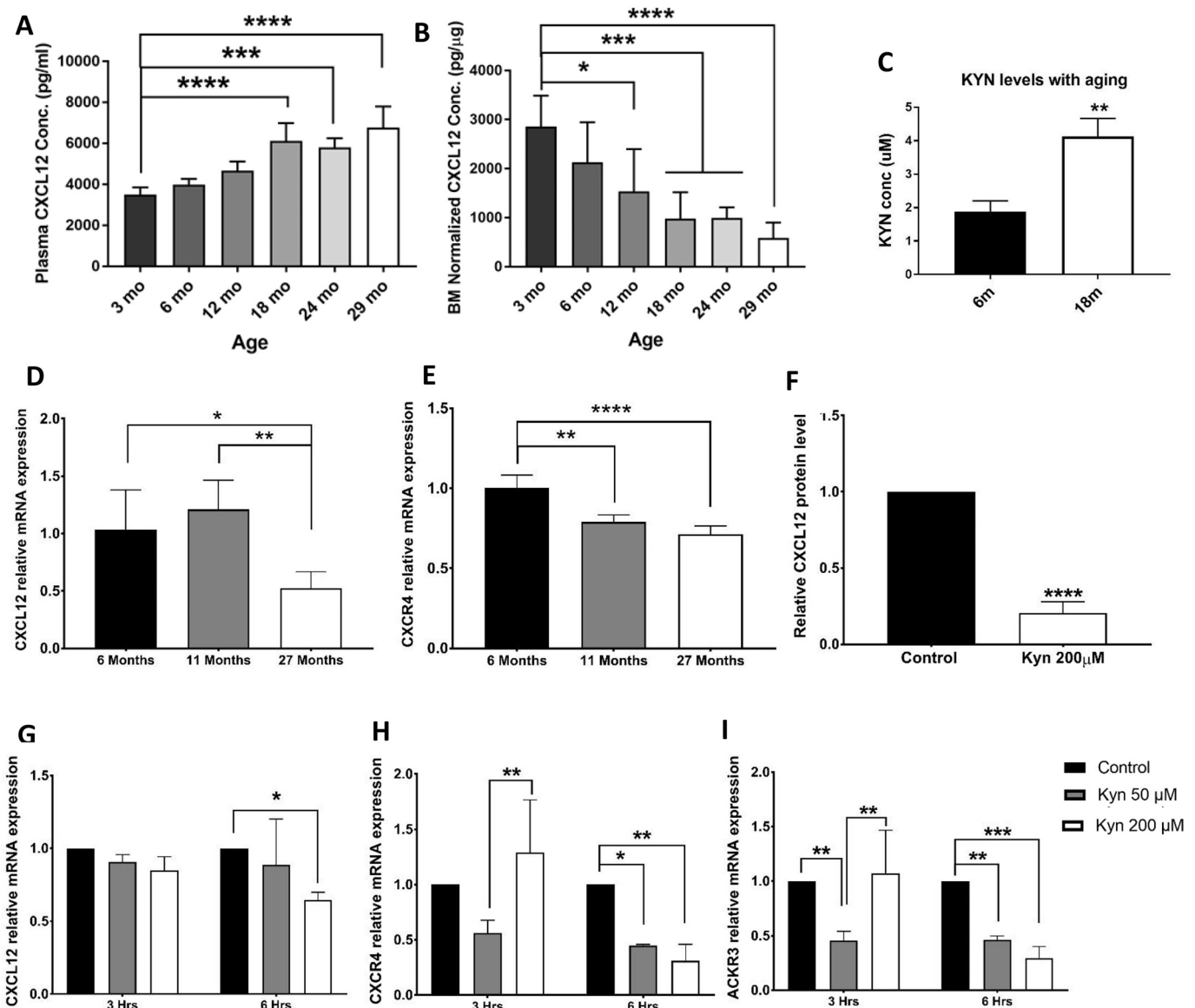


Fig. 1. Aging and kynurenine downregulate CXCL12 axis. (A) CXCL12 protein levels in murine plasma from 3, 6, 12, 18, 24, and 29 months-old mice ($n = 10$). (B) CXCL12 protein levels in murine bone marrow interstitial fluid from 3, 6, 12, 18, 24, and 29 months-old mice ($n = 10$ mice per group). (C) Kynurenine level (μM) in cell culture media of BMSCs isolated from 6 and 18 months old mice ($n = 3$). (D,E) mRNA levels of CXCL12 (D) and CXCR4 (E) in BMSCs isolated from 6, 11, and 27 months-old mice ($n = 4$ for 6 and 11 months old mice and $n = 7$ for 27 months old mice). (F) CXCL12 protein levels in BMSCs isolated from pooled 6 months-old mice after treatment with 200 μM kynurenine for 48 h ($n = 4$). (G-I) mRNA levels of CXCL12 (F), and CXCR4 (G) and ACKR3 (H) after treatment with 50 and 200 μM kynurenine for 6 h ($n = 3$). Data presented as mean \pm SD. Data analysis was done using one way ANOVA for panels A, B, D, E, F, G, H, and I, and using unpaired t -test for panel C. Data presented as mean \pm SD. * $P < 0.05$, ** $P < 0.01$, *** $p < 0.001$, **** $p < 0.0001$.

elderly (27 months), at which time there is significant age-associated bone loss and a significant reduction in BM interstitial fluid CXCL12 (Hamrick et al., 2006; Refaey et al., 2017). CXCL12 mRNA levels significantly declined to 50% at 27 months, while CXCR4 mRNA levels were significantly reduced earlier at both 11 and 27 months of age compared to 6 month-old mice (Figs. 1D, E).

Since KYN levels are linked to aging, we then tested if KYN treatment of BMSCs had a similar effect. BMSCs isolated from 3-, 6-, and 18-month-old mice showed significantly lower CXCL12 protein levels in the cell culture media upon treatment with 200 μM KYN compared to control. CXCL12 protein secreted in culture media from BMSCs isolated from young mice (6 months) was significantly reduced, almost 80%, when treated for 48 h with 200 μM KYN (Fig. 1F). Secretion of CXCL12 from BMSCs of 3 and 18 months old mice was also decreased with KYN (Supp. Figs. 1A,B). Consistently, there was a significant decrease in CXCL12 mRNA expression in the BMSCs as early as 6 h after treatment. Concomitant with reduction in CXCL12 expression, mRNA expression of the receptors, CXCR4 and CXCR7, was also decreased by almost 30–50% (Fig. 1G–I). BMSCs isolated from 6-month-old mice showed similar changes in CXCL12 mRNA expression at later time points with a significant decrease at 48 h post-treatment (Supp. Fig. 1C).

3.2. KYN attenuated osteogenesis and osteogenic gene expression in BMSCs

In vivo experiments have shown that KYN accumulates with aging and induces bone loss (Refaey et al., 2017). To establish if, at least in part, KYN achieves this function via inhibition of BMSC osteogenesis, we treated BMSCs isolated from 6- and 18-month-old mice with different doses of KYN (10, 50, 200 μM). Using osteogenic differentiation media for 21 days and Alizarin Red staining, KYN doses inhibited osteogenic differentiation in BMSCs from 6-month-old mice in a dose dependent manner, with the high KYN dose (200 μM) showing a significant 50% decrease (Fig. 2A). After 14 days, the high KYN dose also showed significant inhibition of mineralization with Alizarin Red

staining (Supp. Fig. 2A), as well as intermittent doses (Supp. Fig. 2D). The early effects of KYN on osteogenic differentiation of BMSCs isolated from 6 months old mice were confirmed using alkaline phosphatase activity assay after 7 days of incubation in osteogenic differentiation media (Fig. 2B). To determine whether this KYN effect was in fact due to inhibition of osteogenesis and not an effect on cell density, a crystal violet assay assessed KYN cytotoxicity and showed that none of the doses of KYN (10, 50, and 200 μM) affected cell proliferation as determined by the number of BMSCs when cultured under the same conditions as the osteogenic differentiation experiments (Supp. Fig. 2C).

Next, directly isolated BMSCs (i.e., without in vitro expansion/passaging prior to experimentation) from young and old mice (6–8 months versus 22–24 months) were used to assess how KYN affects their osteogenic differentiation marker expression. Basal expression level of the osteogenic marker, Runx2 was significantly lower in osteogenically-cultured BMSCs isolated from old mice compared to similarly cultured BMSCs isolated from young mice. We also found that treating BMSCs from either younger or older mice with KYN significantly reduced their mRNA levels of Runx2, resembling the effect of aging. Runx2 protein expression was also significantly downregulated after 7 days of KYN treatment in osteogenic differentiation media (Fig. 2C, D).

3.3. The KYN treatment phenotype resembles aging in upregulating CXCL12-targeting miR-29b-1-5p

To determine how in vitro administration of KYN induced a phenotype reminiscent of organismal aging in terms of miR-29b-1 expression, we measured miR-29b-1-5p levels in BMSCs from young versus old mice. BMSCs isolated from aged mice had significantly higher levels of miR-29b-1-5p and significantly lower levels of miR-29b-1-3p compared to BMSCs from younger mice (Fig. 3A, B). As in the mice we also found that miR-29b-1-5p levels in aged human MSCs were significantly

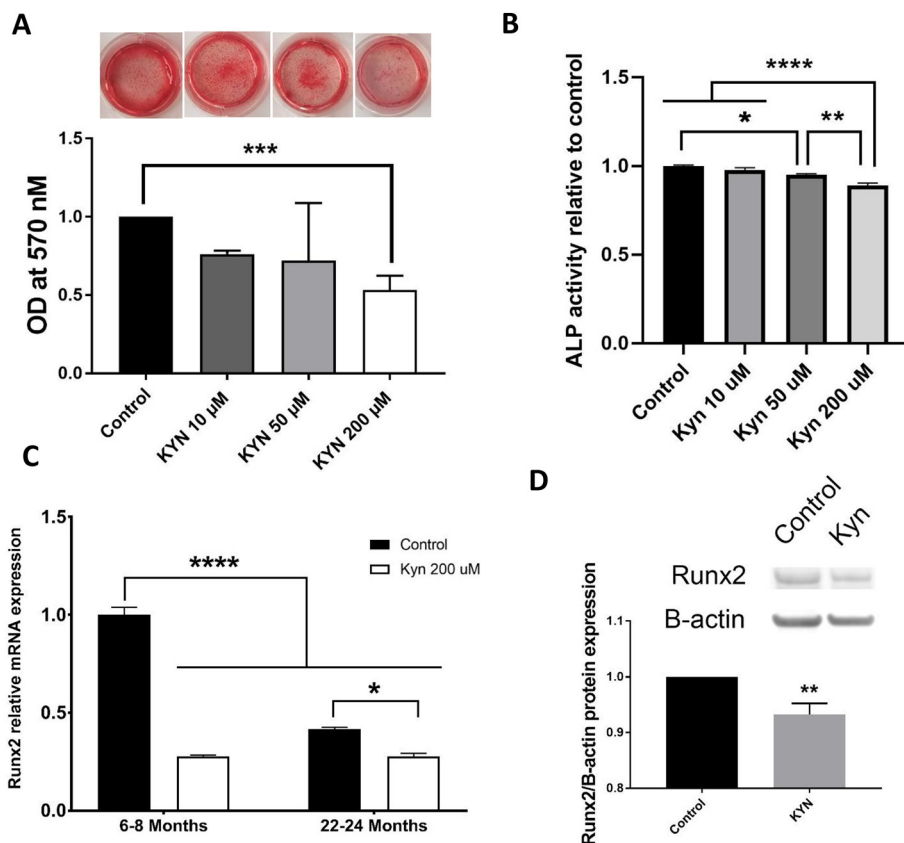


Fig. 2. Kynurenine inhibits BMSCs osteogenic differentiation. (A) Optical density of alizarin red osteogenic assay staining and corresponding wells of BMSCs isolated from pooled 6 months-old mice after treatment with different doses of kynurenine (10, 50, and 200 μM) for 21 days (n = 6). (B) Alkaline Phosphatase (ALP) activity relative to control in BMSCs isolated from pooled 6 months-old mice treated with different doses of kynurenine (10, 50, and 200 μM) for 7 days (n = 6) (C) mRNA levels of Runx2 in BMSCs isolated from young (6–8 months-old) and old (22–24 months-old) mice, in osteogenic differentiation medium with or without 200 μM kynurenine for 7 days (n = 3 mice per group). (D) Protein levels of Runx2 in BMSCs isolated from 6 months mice after incubation in osteogenic differentiation medium with or without 200 μM kynurenine for 7 days. Data presented as mean ± SD. Data analysis was done using one way ANOVA for panels A, B, and C, and using unpaired t-test for panel D. *P < 0.05, **P < 0.01, ***P < 0.001, ****P < 0.0001.

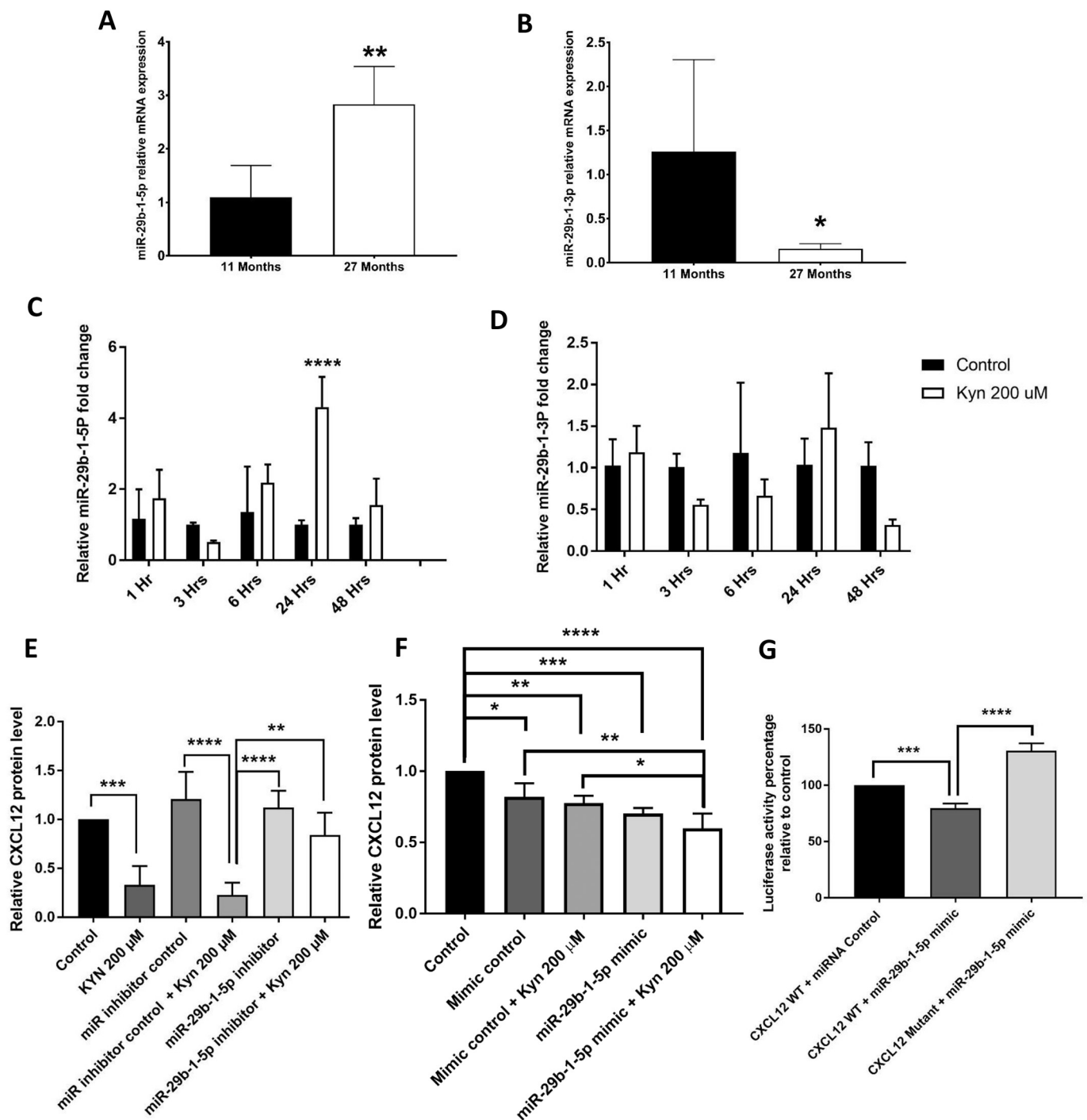


Fig. 3. Kynurenine upregulates pro-aging and CXCL12-targeting miR-29b-1-5p. (A,B) miR-29b-1-5p (A) and miR-29b-1-3p (B) levels in BMSCs isolated from 11 versus 27 months old ($n = 4$ for 11 months old mice and $n = 7$ for 27 months old mice). (C,D) miR-29b-1-5p levels (C) and miR-29b-1-3p levels (D) in BMSCs isolated from pooled 6 months-old mice after treatment with 200 μM kynurenine for 1, 3, 6, 24 and 48 h ($n = 3$). (E,F) CXCL12 levels in BMSCs isolated from 6 months old mice after treatment with 200 μM kynurenine with or without transfection with miR-29b-1-5p inhibitor (E) or miR-29b-1-5p mimic (F) ($n = 8$ for inhibitor and $n = 4$ for mimic). (G) Luciferase activity of CXCL12 reporter plasmids (wild type and mutant) after transfection with miR-29b-1-5p mimic relative to luciferase activity of wild type CXCL12 reporter plasmid after transfection with miRNA mimic control for 24 h ($n = 3$). Data presented as mean \pm SD. Data analysis was done using one way ANOVA for panels E, F and G, using two way ANOVA for panels C and D, and using unpaired t-test for panels A and B. * $P < 0.05$, ** $P < 0.01$, *** $p < 0.001$, **** $p < 0.0001$.

upregulated in aged vs. adult MSCs, but different from the murine the miR-29b-1-3p levels were not significantly changed in humans with age (Supp. Fig. 3A).

We then measured miR-29b-1-5p levels in murine BMSCs from 6-month-old mice with or without KYN treatment for 1, 3, 6, 24, and 48 h. KYN transiently, upregulated miR-29b-1-5p beginning at 24 h (Fig. 3C).

The levels of miR-29b-1-5p expression in response to KYN was almost back to normal by 48 h.

To confirm that increased levels of miR-29b-1-5p mediated KYN's effect on the CXCL12 axis, rather than being an independent downstream effect of KYN, we transfected BMSCs isolated from 6-month-old mice with a miR-29b-1-5p inhibitor, and treated them with KYN for

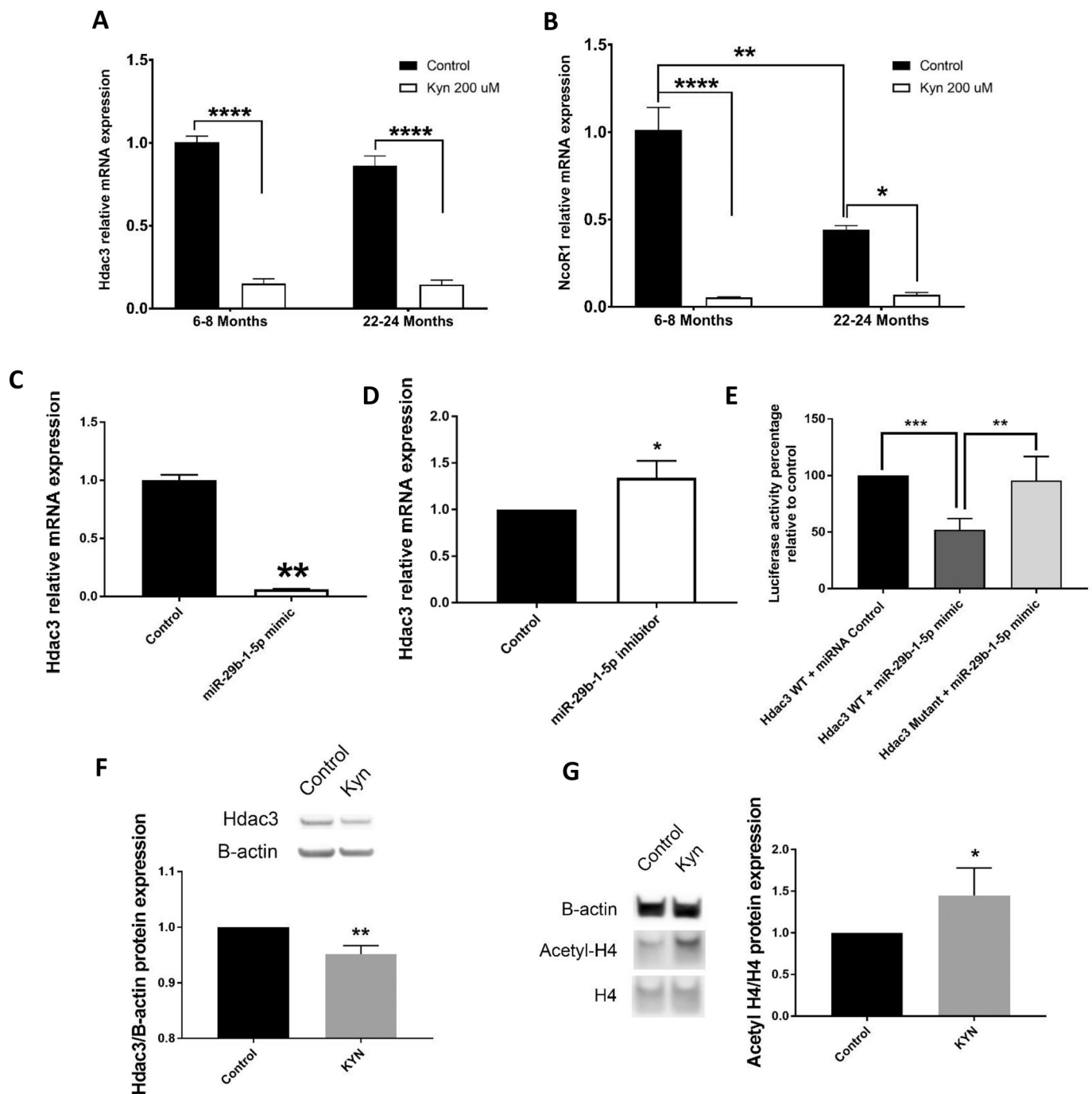


Fig. 4. Kynurenine downregulates Hdac3 and its cofactors. (A,B) mRNA expression levels of (A) Hdac3 and (B) NcoR1 in BMSCs isolated directly from young and old mice and cultured in osteogenic differentiation medium with or without 200 μ M kynurenine for 7 days ($n = 3$). (C,D) mRNA expression levels of Hdac3 in BMSCs isolated from pooled 6 months-old mice and transfected with either (C) miR-29b-1-5p mimic or (D) miR-29b-1-5p inhibitor compared to their respective controls ($n = 3$). (E) Luciferase activity of Hdac3 reporter plasmids (wild type and mutant) after transfection with miR-29b-1-5p mimic relative to luciferase activity of wild type Hdac3 reporter plasmid after transfection with miRNA mimic control for 24 h ($n = 3$). (F,G) Protein levels of Hdac3 (F) and H4 acetylation (G) in BMSCs isolated from pooled 6 months-old mice after incubation in osteogenic differentiation medium with or without 200 μ M kynurenine for 7 days. Data presented as mean \pm SD. Data analysis was done using one way ANOVA for panel E, using two way ANOVA for panels A and B, and using unpaired t-test for panels C, D, F, and G. * $P < 0.05$, ** $P < 0.01$, *** $p < 0.001$, **** $p < 0.0001$.

ratio of bone formation to bone resorption with aging. Osteoporosis is mostly asymptomatic during the first few years which makes early diagnosis more difficult (Phetfong et al., 2016). Currently available treatments for osteoporosis can be associated with a wide range of side effects (Antebi et al., 2014). A key barrier to preventing osteoporosis or developing efficient new treatments is understanding the mechanisms underlying the aging-related deterioration in bone health and

subsequent progression of osteoporosis. Our group and others have demonstrated that osteoporosis is - at least in part - a stem cell disease (Infante and Rodriguez, 2018; Herberg et al., 2015; Antebi et al., 2014). This study aimed to investigate molecular pathways triggering age-associated changes in the bone marrow stem cell populations that could lead to osteoporosis and thus may represent a new therapeutic target.

Osteogenic differentiation is critical in bone aging; as we age, there

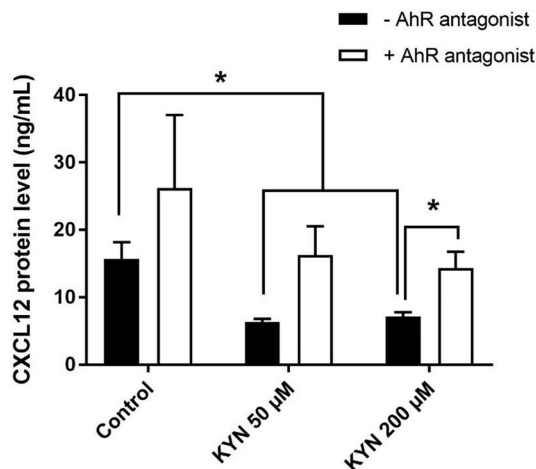


Fig. 5. AhR antagonist inhibits kynurenine-induced CXCL12 downregulation. CXCL12 protein levels in BMSCs isolated from pooled 6-month-old mice after treatment for 48 h with 100 or 200 µM kynurenine with or without 10 µM of AhR-antagonist 3',4'-Dimethoxyflavone (DMF) ($n = 3$). Data presented as mean \pm SD. Data analysis was done using unpaired t-test. $**P < 0.01$.

is a shift in BMSCs from osteogenic to adipogenic differentiation (Infante and Rodriguez, 2018). Our group and other groups have reported the beneficial role of CXCL12 α and β in the osteogenic differentiation of BMSCs (Yang et al., 2018a; Herberg et al., 2014a; Herberg et al., 2015). We have found that increased KYN levels, as well as an elevated KYN to TRP ratio, contribute to reductions in BMSCs osteogenesis and subsequent decreased bone formation in association with aging (El Refaey et al., 2015; Kim et al., 2019). We have previously reported increased serum and bone marrow levels of KYN with aging in humans (Refaey et al., 2017) (Kim et al., 2019). While the specific mechanism of age-related increases in KYN levels in different tissue compartments is still not fully understood, the elevated KYN levels may be due to upregulated local IDO activity with aging, as well as increased ROS mediated conversion of tryptophan to KYN. These, or potentially other mechanisms can lead to higher KYN levels and an increase in the KYN/TRP ratio (Souza et al., 2018; Sas et al., 2018). KYN also downregulates Hdac3 and its cofactor NcoR1 which increases the degree of adiposity in murine bone marrow together with reducing bone mass (Refaey et al., 2017). We also recently assessed an array of miRNAs that are upregulated in human BMSCs with aging, identifying miR-29b-1-5p as a key miRNA involved in inhibiting osteogenesis with age (Hill et al., 2016; Periyasamy-Thandavan et al., 2013; Baglio et al., 2013; Lee et al., 2016; Suh et al., 2013a; Shi et al., 2016; Li et al., 2009; William and Hill, 2016; Periyasamy-Thandavan et al., 2012). Here, we investigate how these different anti-osteogenic pathways interact, underscoring

new biomarkers that can be targeted for clinical intervention to prevent or treat osteoporosis at the stem cell level.

Our results here confirm that KYN inhibits BMSC osteogenesis and downregulates osteogenic gene expression. This is in agreement with work from Dinçel et al., who showed a significant correlation between a high KYN/TRP ratio and the incidence of osteoporotic hip fracture (Dinçel et al., 2017). We have also shown that KYN levels and the KYN/TRP ratio in the human bone marrow microenvironment are increased with age (Kim et al., 2019). More importantly, we showed that subjects with increased bone fragility, marked by decreased total femur BMD and increased markers of bone resorption, have significantly higher KYN levels and KYN/TRP ratios than those without (Kim et al., 2019). Another group demonstrated that high levels of peripheral KYN and AhR are significantly correlated with decreased bone strength, in contrast high central KYN levels in the frontal cortex of the brain are correlated with increased bone strength (Kalaska et al., 2017a; Kalaska et al., 2017b). These investigators believe that similar to serotonin, another TRP metabolite, KYN can exert opposing effects on bone formation depending on its site of action (Kalaska et al., 2017b; Ducey and Karsenty, 2010).

The identification of mechanisms underlying KYN's anti-osteogenic effects has been limited. Here, we demonstrate potential novel mechanisms based on downregulation of CXCL12 axis mRNA expression and protein levels, via KYN ligand signaling through the AhR and mediated by epigenetic changes in miRNAs and Hdac3. The decrease in CXCL12 protein levels in response to KYN treatment and our previous findings indicating that CXCL12 is important for osteogenesis, in turn support the theory that KYN inhibits BMSCs osteogenesis via downregulation of the CXCL12 axis. We also found that KYN-mediated downregulation of CXCL12 mimics the decline in CXCL12 protein levels in human and murine bone marrow interstitial fluid with aging. The reason for the corresponding age-related increase in CXCL12 levels in murine and human plasma is not clear, but it could be due to summing of inflammatory responses throughout the body in the plasma, or to regulated compartmentalized changes in CXCL12 expression that are different in the bone marrow versus plasma, and/or to an accumulation of DPP4-cleaved non-CXCR4-activating CXCL12 in plasma subsequent to feedback (Carbone et al., 2017; Ding et al., 2007; Elmansi et al., 2019). Recently, links between AhR signaling and both CXCR4 and ACKR3 levels have been suggested, where high AhR expression was correlated with high expression of CXCR4 in breast tumors (Vacher et al., 2018), and hepatic toxicity in response to AhR activation was mediated, at least in part, by changes in ACKR3 mRNA levels (Watson et al., 2017). Another potential link between the KYN pathway and the CXCL12 axis, is the reported IDO- and tryptophan-mediated regulation of CXCR4 expression and responsiveness to chemokines in dendritic cells (Hwang et al., 2005).

KYN may achieve its anti-osteogenic effects in part by upregulating

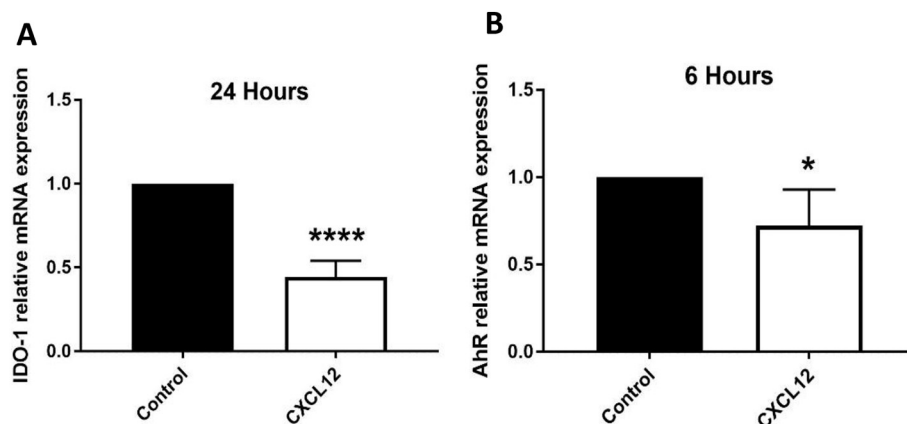


Fig. 6. CXCL12 regulates mRNA levels of IDO-1 and AhR. (A,B) mRNA expression levels of (A) IDO-1, and (B) AhR after treatment with CXCL12 (200 ng/mL) for 24 and 6 h respectively ($n = 4$). Data presented as mean \pm SD. Data analysis was done using one way ANOVA for panel C, and using unpaired t-test for panels A and B. $*P < 0.05$, $***p < 0.001$, $****p < 0.0001$.

miR-29b-1-5p, which targets CXCL12 and other osteogenic genes. We noticed that changes in miR-29b-1-5p in response to KYN treatment of 200 μ M peaked around 24 h and was almost back to basal level by 48 h, which is expected due to the transient on/off nature of miRNA regulation (Bail et al., 2010; Zhang et al., 2012; R uegger and Gro shans, 2012). This miRNA upregulation supports the idea that increased KYN levels with age may be a key regulator of the age-associated decrease in osteogenesis. In this study, we focused mainly on miR-29b-1-5p since, it targeted both CXCL12 and Hdacs, a second distinct epigenetic regulatory system. We had in silico evidence that miR-29b-1-5p targets position 278–302 of the Hdac3 3' UTR (Miranda et al., 2006). We confirmed here, for the first time that this miRNA directly targets and down-regulates both Hdac3 and CXCL12. Whether KYN can down-regulate CXCL12 independently from miR-29b-1-5p is yet to be determined. We found that KYN's effect on the CXCL12 protein level is attenuated by the use of a miR-29b-1-5p (antagomir) inhibitor and increased by the use of the miR-29b-1-5p mimic. This is further evidence that miR-29b-1-5p is involved in KYN's downregulation of CXCL12. This age-associated miRNA upregulation supports the idea that increased KYN levels with age may be a key regulator of the age-associated decrease in osteogenesis and may be linked to aging in other systems.

The effect of KYN on miR-29b-1-5p supports results from other groups that miR-29b may play a role in osteoarthritis development through inhibiting the expression of collagen I by chondrocytes and collagen III by BMSCs (Mayer et al., 2017). We also found that miR-29b-1-5p and miR-29b-1-3p levels change in opposite directions in mice with aging. This is interesting, because Feichtinger et al. (Feichtinger et al., 2018) found that high levels of miR-29b-1-3p are associated with healthy bone microstructure and histomorphometry. In previous work on human BMSCs, we only observed an increase in the miR-29b-1-5p

passenger strand with aging without a concomitant decrease in the miR-29b-1-3p guide strand (Supp. Fig. 3C) (Periyasamy-Thandavan et al., 2012); thus, there may be a difference between human and murine age-associated expression of the guide and passenger strand levels with the regulation of the 5p arm being more critical in aging humans. miR-29b is not the only miRNA bone marker that shows opposing effects of its guide and passenger strands on bone health, as miR-500a-3p was shown to have a positive correlation with bone surface, as well as mineral apposition rate, while miR-500a-5p was shown to play an inhibitory role in osteogenic differentiation and was reported as a novel biomarker for fracture risk in postmenopausal women (Feichtinger et al., 2018; Heilmeier et al., 2016). These observations support the idea that in pathologies, including aging, there may be a dysregulation of the microRNA processing leading to significant changes in the targeting of mRNAs.

Importantly, KYN also downregulates Hdac3 and its cofactor NcoR1; an effect that we previously linked to decreased osteogenesis and increased adipogenesis in murine bone marrow (Refaey et al., 2017; Razidlo et al., 2010). Hdac3 plays a critical role in the process of endochondral ossification and bone matrix remodeling. Loss of Hdac3 in osteochondral progenitors leads to an osteopenic phenotype from impaired bone formation and increasing marrow adiposity, and postnatal inducible conditional knockout of chondrocyte Hdac3 leads to several skeletal abnormalities as well as increased osteoclastogenesis (Razidlo et al., 2010; Carpio et al., 2016; Gordon et al., 2015; Feigensohn et al., 2017; McGee-Lawrence et al., 2016). These studies all implicate Hdac3 as a crucial mediator of endochondral ossification, particularly in the context of aging. It is also important to note that Hdac3 plays an important role in adipogenesis, where lower Hdac3 levels correlated with an increase in bone marrow fat (Razidlo et al., 2010). This effect could explain the increase in bone marrow adipose tissue we previously

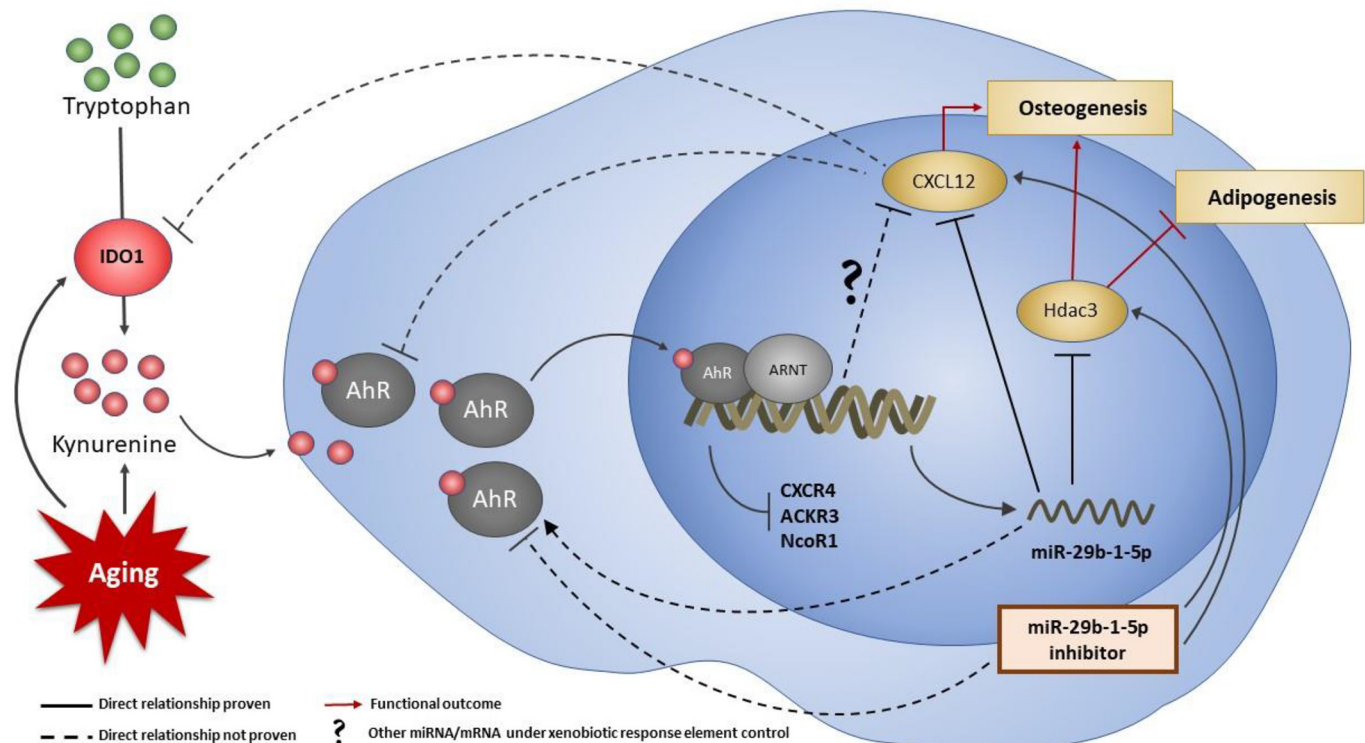


Fig. 7. Proposed pathway of kynurenine effects on BMSCs. Aging upregulates activity of IDO1 which converts tryptophan to kynurenine. Kynurenine is then taken up by BMSCs and binds to cytoplasmic AhR. Upon binding, ligand-bound AhR is transported into the nucleus where it forms a complex with Aryl hydrocarbon receptor nuclear translocator (ARNT). The newly formed complex acts as a transcription factor and downregulates Hdac3 and CXCL12 transcription while upregulating miR-29b-1-5p. Hence, the overall effect of kynurenine and AhR complex is shifting from osteogenic to adipogenic differentiation in BMSCs. CXCL12 acts via a feedback regulation mechanism to downregulate IDO1 and AhR mRNA levels, while miR-29b-1-5p upregulates AhR mRNA level.

reported in mice that received a high KYN diet (Refaey et al., 2017).

We believe that the effects of KYN reported here are primarily, but not necessarily exclusively, mediated through AhR mediated signaling. In other work, it was demonstrated that AhR activation can affect bone health through downstream effects including reduced ossification as well as inhibition of osteogenic differentiation and osteoblast functions (Yun et al., 2018; Jamsa et al., 2001; Milbrath et al., 2009). Here, we found that the use of the AhR antagonists DMF and CH-223192 in combination with KYN partially rescued CXCL12 gene and protein expression. The anti-osteogenic action of KYN may be mediated through other pathways as well. Indeed, it was recently reported that KYN can regulate Wnt signaling and inhibit β -catenin expression, which is a key regulatory pathway for osteogenesis and bone formation (Park et al., 2018), and miR-29b-1-5p is predicted to potentially target Wnt1. Furthermore, the miR-29b-1-5p mimic significantly upregulated AhR mRNA expression levels, while both the miR-29b-1-5p inhibitor and CXCL12 significantly downregulated those levels and CXCL12 also downregulated IDO-1 expression. This result suggests that either miR-29b-1-5p is upstream of AhR activation, or a feedback regulation mechanism exists between the two, as well as cross-talk between CXCL12 with IDO-1 and AhR, as well as being potentially able to target multiple osteogenic genes. (Fig. 7).

In summary, we show that KYN contributes to bone aging via AhR activation, which leads to upregulation of miR-29b-1-5p with down-regulation of both Hdac3 and CXCL12. These combined effects lead to a reduced osteogenic differentiation capacity in BMSCs, and contributes to the aging-induced decline in bone formation. Whether the effects of KYN are solely mediated via AhR is yet to be determined. We believe that KYN pathway mediators including IDO-1 and AhR, as well as the downstream molecules investigated in this work (CXCL12, Hdac3, and miR29b-1-5p), offer new potential targets for clinical intervention to prevent or treat osteoporosis.

Declaration of competing interest

Drs. William Hill, Sergio Mas Herrero, and Sudharsan Periyasamy-Thanavanis are inventors on U.S. Patent No. 9,267,139, "Compositions and Methods for Treating Musculoskeletal Disorders" issued. Ahmed Elmansi, Galina Kondrikova, Jessica Pierce, Helen Kaiser, Drs. Khaled Hussein, Xue Jiang, Alexandra Aguilar-Pérez, Dmitry Kondrikov, Nada H. Eisa, Ke-Hong Ding, Aisha Walker, Sadanand Fulzele, Wendy B. Bollag, Mohammed Elsalanty, Qing Zhong, Xing-ming Shi, Yun Su, Maribeth Johnson, Monte Hunter, Charles Reitman, Brian Volkman, Mark Hamrick, Carlos Isales, Meghan McGee-Lawrence have no conflicts of interest or financial ties to disclose.

Acknowledgments

This publication is based upon work supported in part by the Department of Veterans Affairs, Veterans Health Administration Office of Research and Development, Clinical Science Research and Development Program (VA Merit Award 1101CX000930-01, WDH) and the National Institutes of Health (NIA-AG036675 SF, MWH, CMI, MM-L, and WDH). The contents of this publication do not represent the views of the Department of Veterans Affairs, or the United States Government.

Authors' roles

Study design: KAH, AME, MM-L, and WDH. Study conduct: AME, KAH, SMH, SP-T, NHE, XJ, AA-P, ALW, X-MS, YS, and HK. Data collection: AME, SMH, NHE, GK, JP, and ALW. Data analysis: SMH, KAH, AME, WDH and MM-L. Statistical Analysis: AME, KAH, and MJ. Data interpretation: AME, SMH, SF, WBB, WDH, MM-L. Drafting manuscript: AME, KAH and WDH. Revising manuscript content: K-HD, ME, QZ, X-

MS, MH, MWH, CR, BFV, SF, DK, CMI, MM-L, and WDH. Approving final version of manuscript: MWH, CMI, SF, MM-L, and WDH. MM-L and WDH take responsibility for the integrity of the data analysis.

Appendix A. Supplementary data

Supplementary data to this article can be found online at <https://doi.org/10.1016/j.bonr.2020.100270>.

References

- Álvarez-Viejo, M., 2015. CD271 as a marker to identify mesenchymal stem cells from diverse sources before culture. *World Journal of Stem Cells* 7 (2), 470.
- Antebi, B., Pelled, G., Gazit, D., 2014. Stem cell therapy for osteoporosis. *Current osteoporosis reports* 12 (1), 41–47.
- Apalset, E.M., Gjesdal, C.G., Ueland, P.M., Midttun, Ø., Ulvik, A., Eide, G.E., et al., 2014. Interferon (IFN)- γ -mediated inflammation and the kynurenine pathway in relation to bone mineral density: the Hordaland Health Study. *Clinical & Experimental Immunology* 176 (3), 452–460.
- Asai, H., Hirata, J., Watanabe-Akanuma, M., 2018. Indoxyl glucuronide, a protein-bound uremic toxin, inhibits hypoxia-inducible factor–dependent erythropoietin expression through activation of aryl hydrocarbon receptor. *Biochem. Biophys. Res. Commun.* 504 (2), 538–544.
- Baglio, S.R., Devescovi, V., Granchi, D., Baldini, N., 2013. MicroRNA expression profiling of human bone marrow mesenchymal stem cells during osteogenic differentiation reveals Osterix regulation by miR-31. *Gene* 527 (1), 321–331.
- Bail, S., Swerdel, M., Liu, H., Jiao, X., Goff, L.A., Hart, R.P., et al., 2010. Differential regulation of microRNA stability. *RNA (New York, NY)* 16 (5), 1032–1039.
- Beischlag, T.V., Luis Morales, J., Hollingshead, B.D., Perdew, G.H., 2008. The aryl hydrocarbon receptor complex and the control of gene expression. *Crit. Rev. Eukaryot. Gene Expr.* 18 (3), 207–250.
- Betel, D., Koppal, A., Agius, P., Sander, C., Leslie, C., 2010. Comprehensive modeling of microRNA targets predicts functional non-conserved and non-canonical sites. *Genome Biol.* 11 (8), R90.
- Bradley, E.W., McGee-Lawrence, M.E., Westendorf, J.J., 2011. Hdac-mediated control of endochondral and intramembranous ossification. *Crit. Rev. Eukaryot. Gene Expr.* 21 (2), 101–113.
- Bromage, D.I., Davidson, S.M., Yellon, D.M., 2014. Stromal derived factor 1 α : a chemokine that delivers a two-pronged defence of the myocardium. *Pharmacol. Ther.* 143 (3), 305–315.
- Brooks, A.K., Lawson, M.A., Smith, R.A., Janda, T.M., Kelley, K.W., McCusker, R.H., 2016. Interactions between inflammatory mediators and corticosteroids regulate transcription of genes within the kynurenine pathway in the mouse hippocampus. *J. Neuroinflammation* 13 (1).
- Broxmeyer, H.E., Orschell, C.M., Clapp, D.W., Hangoc, G., Cooper, S., Plett, P.A., et al., 2005. Rapid mobilization of murine and human hematopoietic stem and progenitor cells with AMD3100, a CXCR4 antagonist. *J. Exp. Med.* 201 (8), 1307–1318.
- Cao, J., Ou, G., Yang, N., Ding, K., Cream, B.E., Hamrick, M.W., et al., 2015. Impact of targeted PPAR γ disruption on bone remodeling. *Mol. Cell. Endocrinol.* 410, 27–34.
- Carbone, L., Buzkova, P., Fink, H., Robbins, J., Bethel, M., Hamrick, M.W., et al., 2017. Association of plasma SDF-1 with bone mineral density, body composition and hip fractures in older adults: the cardiovascular health study. *Calcif. Tissue Int.* 100, 599–608.
- Carpio, L.R., Bradley, E.W., McGee-Lawrence, M.E., Weivoda, M.M., Poston, D.D., Dudakovic, A., et al., 2016. Histone deacetylase 3 supports endochondral bone formation by controlling cytokine signaling and matrix remodeling. *Sci. Signal.* 9 (440), ra79.
- Chen, Q., Shou, P., Zheng, C., Jiang, M., Cao, G., Yang, Q., et al., 2016. Fate decision of mesenchymal stem cells: adipocytes or osteoblasts? *Cell Death & Differentiation* 23 (7), 1128–1139.
- Cheng, A.M., Byrom, M.W., Shelton, J., Ford, L.P., 2005. Antisense inhibition of human miRNAs and indications for an involvement of miRNA in cell growth and apoptosis. *Nucleic Acids Res.* 33 (4), 1290–1297.
- Cheng, X., Wang, H., Zhang, X., Zhao, S., Zhou, Z., Mu, X., et al., 2017. The role of SDF-1/CXCR4/CXCR7 in neuronal regeneration after cerebral ischemia. *Front. Neurosci.* 11, 590.
- Coipeau, P., Rosset, P., Langonné, A., Gaillard, J., Delorme, B., Rico, A., et al., 2009. Impaired differentiation potential of human trabecular bone mesenchymal stromal cells from elderly patients. *Cytotherapy* 11 (5), 584–594.
- Cox, G., Boxall, S.A., Giannoudis, P.V., Buckley, C.T., Roshdy, T., Churchman, S.M., et al., 2012. High abundance of CD271 + multipotential stromal cells (MSCs) in intramedullary cavities of long bones. *Bone* 50 (2), 510–517.
- Cuthbert, R.J., Giannoudis, P.V., Wang, X.N., Nicholson, L., Pawson, D., Lubenko, A., et al., 2015. Examining the feasibility of clinical grade CD271 + enrichment of mesenchymal stromal cells for bone regeneration. *PLoS One* 10 (3), e0117855.
- Dincel, E., Ozkan, Y., Sukuroglu, M., Ozsoy, H., Sepici Dincel, A., 2017. Evaluation of tryptophan/kynurenine pathway relevance with immune system biomarkers of low energy trauma hip fractures in osteoporotic patients. *Archives of rheumatology* 32 (3), 203–208.
- Ding, K.-H., Shi, X.-M., Zhong, Q., Kang, B., Xie, D., Bollag, W.B., et al., 2007. Impact of glucose-dependent insulinotropic peptide on age-induced bone loss. *J. Bone Miner. Res.* 23 (4), 536–543.

- Duan, Z., Li, L., Li, Y., 2019. Involvement of miR-30b in kynurenine-mediated lysyl oxidase expression. *J. Physiol. Biochem.* 75 (2), 135–142.
- Ducy, P., Karsenty, G., 2010. The two faces of serotonin in bone biology. *J. Cell Biol.* 191 (1), 7–13.
- El Refaey, M., Watkins, C.P., Kennedy, E.J., Chang, A., Zhong, Q., Ding, K.-H., et al., 2015. Oxidation of the aromatic amino acids tryptophan and tyrosine disrupts their anabolic effects on bone marrow mesenchymal stem cells. *Mol. Cell. Endocrinol.* 410, 87–96.
- Elmansi, A.M., Awad, M.E., Eisa, N.H., Kondrikov, D., Hussein, K.A., Aguilar-Pérez, A., et al., 2019. What doesn't kill you makes you stranger: Dipeptidyl peptidase-4 (CD26) proteolysis differentially modulates the activity of many peptide hormones and cytokines generating novel cryptic bioactive ligands. *Pharmacol. Ther.* 198, 90–108.
- Farina, N.H., Wood, M.E., Perrapato, S.D., Francklyn, C.S., Stein, G.S., Stein, J.L., et al., 2014. Standardizing analysis of circulating microRNA: clinical and biological relevance. *J. Cell. Biochem.* 115 (5), 805–811.
- Feichtinger, X., Muschitz, C., Heimel, P., Baierl, A., Fahrleitner-Pammer, A., Redl, H., et al., 2018. Bone-related circulating microRNAs miR-29b-3p, miR-550a-3p, and miR-324-3p and their association to bone microstructure and histomorphometry. *Sci. Rep.* 8 (1), 4867.
- Feigenson, M., Shull, L.C., Taylor, E.L., Camilleri, E.T., Riester, S.M., van Wijnen, A.J., et al., 2017. Histone deacetylase 3 deletion in mesenchymal progenitor cells hinders long bone development. *Journal of bone and mineral research : the official journal of the American Society for Bone and Mineral Research* 32 (12), 2453–2465.
- Goldar, S., Khaniani, M.S., Derakhshan, S.M., Baradaran, B., 2015. Molecular mechanisms of apoptosis and roles in cancer development and treatment. *Asian Pacific journal of cancer prevention : APJCP* 16 (6), 2129–2144.
- Gordon, J.A.R., Stein, J.L., Westendorf, J.J., van Wijnen, A.J., 2015. Chromatin modifiers and histone modifications in bone formation, regeneration, and therapeutic intervention for bone-related disease. *Bone* 81, 739–745.
- Granero-Moltó, F., Weis, J.A., Miga, M.I., Landis, B., Myers, T.J., O'Rear, L., et al., 2009. Regenerative effects of transplanted mesenchymal stem cells in fracture healing. *Stem Cells* 27 (8), 1887–1898.
- Gregory, C.A., Gunn, W.G., Peister, A., Prockop, D.J., 2004. An Alizarin red-based assay of mineralization by adherent cells in culture: comparison with cetylpyridinium chloride extraction. *Anal. Biochem.* 329 (1), 77–84.
- Hamrick, M.W., Ding, K.-H., Pennington, C., Chao, Y.J., Wu, Y.-D., Howard, B., et al., 2006. Age-related loss of muscle mass and bone strength in mice is associated with a decline in physical activity and serum leptin. *Bone* 39 (4), 845–853.
- Heilmeyer, U., Hackl, M., Skalicky, S., Weilner, S., Schroeder, F., Vierlinger, K., et al., 2016. Serum miRNA signatures are indicative of skeletal fractures in postmenopausal women with and without type 2 diabetes and influence osteogenic and adipogenic differentiation of adipose tissue-derived mesenchymal stem cells in vitro. *Journal of bone and mineral research : the official journal of the American Society for Bone and Mineral Research* 31 (12), 2173–2192.
- Herberg, S., Fulzele, S., Yang, N.L., Shi, X.M., Hess, M., Periyasamy-Thandavan, S., et al., 2013. Stromal cell-derived Factor-1 beta potentiates bone morphogenetic Protein-2-stimulated osteoinduction of genetically engineered bone marrow-derived mesenchymal stem cells in vitro. *Tissue Eng. A* 19 (1–2), 1–13.
- Herberg, S., Susin, C., Pelaez, M., Howie, R.N., Moreno de Freitas, R., Lee, J., et al., 2014a. Low-dose bone morphogenetic protein-2/stromal cell-derived factor-1beta cotherapy induces bone regeneration in critical-size rat calvarial defects. *Tissue Eng Part A* 20 (9–10), 1444–1453.
- Herberg, S., Kondrikova, G., Hussein, K.A., Periyasamy-Thandavan, S., Johnson, M.H., Elsalanty, M.E., et al., 2014b. Total body irradiation is permissive for mesenchymal stem cell-mediated new bone formation following local transplantation. *Tissue Eng. A* 20 (23–24), 3212–3227.
- Herberg, S., Kondrikova, G., Hussein, K.A., Johnson, M.H., Elsalanty, M.E., Shi, X., et al., 2015. Mesenchymal stem cell expression of stromal cell-derived factor-1β augments bone formation in a model of local regenerative therapy. *Journal of orthopaedic research : official publication of the Orthopaedic Research Society* 33 (2), 174–184.
- Hill, W.D., Periyasami-Thandavan, S., Samuel, H., Inventors; Augusta University, Assignee, 2016. Compositions and Methods for Treating Musculoskeletal Disorders. USA.
- Hwang, S.L., Chung, N.P., Chan, J.K., Lin, C.L., 2005. Indoleamine 2,3-dioxygenase (IDO) is essential for dendritic cell activation and chemotactic responsiveness to chemokines. *Cell Res.* 15 (3), 167–175.
- Infante, A., Rodriguez, C.I., 2018. Osteogenesis and aging: lessons from mesenchymal stem cells. *Stem Cell Res Ther* 9 (1), 244.
- Jamsa, T., Viluksela, M., Tuomisto, J.T., Tuomisto, J., Tuukkanen, J., 2001. Effects of 2,3,7,8-tetrachlorodibenzo-p-dioxin on bone in two rat strains with different aryl hydrocarbon receptor structures. *Journal of bone and mineral research : the official journal of the American Society for Bone and Mineral Research* 16 (10), 1812–1820.
- Kalaska, B., Pawlak, K., Domaniewski, T., Oksztulska-Kolanek, E., Znorko, B., Roszczenko, A., et al., 2017a. Elevated levels of peripheral kynurenine decrease bone strength in rats with chronic kidney disease. *Front. Physiol.* 8, 836.
- Kalaska, B., Pawlak, K., Oksztulska-Kolanek, E., Domaniewski, T., Znorko, B., Karbowska, M., et al., 2017b. A link between central kynurenine metabolism and bone strength in rats with chronic kidney disease. *PeerJ* 5, e3199.
- Kawasaki, H., Chang, H.W., Tseng, H.C., Hsu, S.C., Yang, S.J., Hung, C.H., et al., 2014. A tryptophan metabolite, kynurenine, promotes mast cell activation through aryl hydrocarbon receptor. *Allergy* 69 (4), 445–452.
- Khordadmehr, M., Shahbazi, R., Ezzati, H., Jigari-Asl, F., Sadreddini, S., Baradaran, B., 2019. Key microRNAs in the biology of breast cancer; emerging evidence in the last decade. *J. Cell. Physiol.* 234 (6), 8316–8326.
- Kim, J., Ko, J., 2014. A novel PPARγ2 modulator sLZIP controls the balance between adipogenesis and osteogenesis during mesenchymal stem cell differentiation. *Cell Death & Differentiation* 21 (10), 1642–1655.
- Kim, S.W., Lu, Y., Williams, E.A., Lai, F., Lee, J.Y., Enishi, T., et al., 2017. Sclerostin antibody administration converts bone lining cells into active osteoblasts. *J. Bone Miner. Res.* 32 (5), 892–901.
- Kim, B.J., Hamrick, M.W., Yoo, H.J., Lee, S.H., Kim, S.J., Koh, J.M., et al., 2019. The detrimental effects of Kynurenine, a tryptophan metabolite, on human bone metabolism. *J. Clin. Endocrinol. Metab.* 104, 2334–2342.
- Kuçi, S., Kuçi, Z., Schäfer, R., Spohn, G., Winter, S., Schwab, M., et al., 2019. Molecular signature of human bone marrow-derived mesenchymal stromal cell subsets. *Sci. Rep.* 9 (1).
- Kureel, J., Dixit, M., Tyagi, A.M., Mansoori, M.N., Srivastava, K., Raghuvanshi, A., et al., 2014. miR-542-3p suppresses osteoblast cell proliferation and differentiation, targets BMP-7 signaling and inhibits bone formation. *Cell Death Dis.* 5, e1050.
- Kurz, K., Herold, M., Winkler, C., Klotz, W., Russe, E., Fuchs, D., 2011. Effects of adalimumab therapy on disease activity and interferon-gamma-mediated biochemical pathways in patients with rheumatoid arthritis. *Autoimmunity* 44 (3), 235–242.
- Lee, Y., Kim, H.J., Park, C.K., Kim, Y.G., Lee, H.J., Kim, J.Y., et al., 2013. MicroRNA-124 regulates osteoclast differentiation. *Bone* 56 (2), 383–389.
- Lee, W.Y., Li, N., Lin, S., Wang, B., Lan, H.Y., Li, G., 2016. miRNA-29b improves bone healing in mouse fracture model. *Mol. Cell. Endocrinol.* 430, 97–107.
- Lee, W.-C., Guntur, A.R., Long, F., Rosen, C.J., 2017. Energy metabolism of the osteoblast: implications for osteoporosis. *Endocr. Rev.* 38 (3), 255–266.
- Letterova, M.L., Zhang, Y., Steger, D.J., Schupp, M., Schug, J., Cristancho, A., et al., 2008. PPAR and C/EBP factors orchestrate adipocyte biology via adjacent binding on a genome-wide scale. *Genes Dev.* 22 (21), 2941–2952.
- Li, G., Basu, S., Han, M.-K., Kim, Y.-J., Broxmeyer, H.E., 2007. Influence of ERK activation on decreased chemotaxis of mature human cord blood monocyte-derived dendritic cells to CCL19 and CXCL12. *Blood* 109 (8), 3173–3176.
- Li, Z., Hassan, M.Q., Jafferji, M., Aqeilan, R.I., Garzon, R., Croce, C.M., et al., 2009. Biological functions of miR-29b contribute to positive regulation of osteoblast differentiation. *J. Biol. Chem.* 284 (23), 15676–15684.
- Lob, S., Konigsrainer, A., Zieker, D., Brucher, B.L., Rammensee, H.G., Opelz, G., et al., 2009. IDO1 and IDO2 are expressed in human tumors: levo- but not dextro-1-methyl tryptophan inhibits tryptophan catabolism. *Cancer immunology, immunotherapy : CII* 58 (1), 153–157.
- López-Otín, C., Blasco, M.A., Partridge, L., Serrano, M., Kroemer, G., 2013. The hallmarks of aging. *Cell* 153 (6), 1194–1217.
- Manolagas, S.C., 2000. Birth and death of bone cells: basic regulatory mechanisms and implications for the pathogenesis and treatment of osteoporosis. *Endocr. Rev.* 21 (2), 115–137.
- Manolagas, S.C., Parfitt, A.M., 2010. What old means to bone. *Trends in Endocrinology & Metabolism* 21 (6), 369–374.
- Matic, I., Matthews, B.G., Wang, X., Dymont, N.A., Worthley, D.L., Rowe, D.W., et al., 2016. Quiescent bone lining cells are a major source of osteoblasts during adulthood. *Stem Cells* 34 (12), 2930–2942.
- Mayer, U., Benditz, A., Grassel, S., 2017. miR-29b regulates expression of collagens I and III in chondrogenically differentiating BMSC in an osteoarthritic environment. *Sci. Rep.* 7 (1), 13297.
- McGee-Lawrence, M.E., Carpio, L.R., Schulze, R.J., Pierce, J.L., McNiven, M.A., Farr, J.N., et al., 2016. Hdac3 deficiency increases marrow adiposity and induces lipid storage and glucocorticoid metabolism in osteochondroprogenitor cells. *Journal of bone and mineral research : the official journal of the American Society for Bone and Mineral Research* 31 (1), 116–128.
- Merlo, L.M.F., Mandik-Nayak, L., 2016. IDO2: a pathogenic mediator of inflammatory autoimmunity. *Clinical medicine insights Pathology* 9 (Suppl. 1), 21–28.
- Metz, R., Smith, C., DuHadaway, J.B., Chandler, P., Baban, B., Merlo, L.M.F., et al., 2014. IDO2 is critical for IDO1-mediated T-cell regulation and exerts a non-redundant function in inflammation. *Int. Immunol.* 26 (7), 357–367.
- Mezrich, J.D., Fechner, J.H., Zhang, X., Johnson, B.P., Burlingham, W.J., Bradfield, C.A., 2010. An interaction between kynurenine and the aryl hydrocarbon receptor can generate regulatory T cells. *Journal of immunology (Baltimore, Md. : 1950)* 185 (6), 3190–3198.
- Milbrath, M.O., Wenger, Y., Chang, C.W., Emond, C., Garabrant, D., Gillespie, B.W., et al., 2009. Apparent half-lives of dioxins, furans, and polychlorinated biphenyls as a function of age, body fat, smoking status, and breast-feeding. *Environ. Health Perspect.* 117 (3), 417–425.
- Miranda, K.C., Huynh, T., Tay, Y., Ang, Y.-S., Tam, W.-L., Thomson, A.M., et al., 2006. A pattern-based method for the identification of microRNA binding sites and their corresponding heteroduplexes. *Cell* 126 (6), 1203–1217.
- Mortensen, L.J., Hill, W.D., 2015. Skeletal stem cells for bone development, homeostasis and repair: one or many? *Bonekey Rep* 4, 769.
- Murray, I.A., Patterson, A.D., Perdew, G.H., 2014. Aryl hydrocarbon receptor ligands in cancer: friend and foe. *Nat. Rev. Cancer* 14 (12), 801–814.
- Opitz, C.A., Litzenburger, U.M., Sahm, F., Ott, M., Tritschler, I., Trump, S., et al., 2011. An endogenous tumour-promoting ligand of the human aryl hydrocarbon receptor. *Nature* 478 (7368), 197–203.
- Park, J.H., Lee, J.M., Lee, E.J., Kim, D.J., Hwang, W.B., 2018. Kynurenine promotes the goblet cell differentiation of HT-29 colon carcinoma cells by modulating Wnt, Notch and AhR signals. *Oncol. Rep.* 39 (4), 1930–1938.
- Periyasamy-Thandavan, S.M., Fulzele, S., Hamrick, M.W., Shi, X.-M., Isales, C.M., Chutkan, N., Ruark, R., Hinson, J., Hunter, M., Corpe, R., Xu, H., Hill, W.D., 2012. Differential Expression of MicroRNAs in Human Mesenchymal Stem Cells With Age May Be Related to Musculoskeletal Disorders. *ASBMR, Minneapolis, USA.*
- Periyasamy-Thandavan, S., Mas, S., Fulzele, S., Shi, X.M., Chutkan, N., Ruark, R., et al., 2013. Age-associated changes in MicroRNA expression affects differentiation potential in human mesenchymal stem cells. *JBMR* 28, SA0002 Sup 1.

- Periyasamy-Thandavan, S., Burke, J., Mendhe, B., Kondrikova, G., Kolhe, R., Hunter, M., et al., 2018. MicroRNA-141-3p negatively modulates SDF-1 expression in age-dependent pathophysiology of human and murine bone marrow stromal cells. *The Journals of Gerontology: Series A* 74, 1368–1374.
- Phetfong, J., Sanvoranart, T., Nartprayut, K., Nimsanor, N., Seenprachawong, K., Prachayasittikul, V., et al., 2016. Osteoporosis: the current status of mesenchymal stem cell-based therapy. *Cellular & molecular biology letters* 21, 12.
- Platten, M., Nollen, E.A.A., Röhrig, U.F., Fallarino, F., Opitz, C.A., 2019. Tryptophan metabolism as a common therapeutic target in cancer, neurodegeneration and beyond. *Nat. Rev. Drug Discov.* 18 (5), 379–401.
- Poloni, A., Maurizi, G., Rosini, V., Mondini, E., Mancini, S., Discepoli, G., et al., 2009. Selection of CD271+ cells and human AB serum allows a large expansion of mesenchymal stromal cells from human bone marrow. *Cytotherapy* 11 (2), 153–162.
- Quinn, K.E., Mackie, D.I., Caron, K.M., 2018. Emerging roles of atypical chemokine receptor 3 (ACKR3) in normal development and physiology. *Cytokine* 109, 17–23.
- Razidlo, D.F., Whitney, T.J., Casper, M.E., McGee-Lawrence, M.E., Stensgard, B.A., Li, X., et al., 2010. Histone deacetylase 3 depletion in osteo/chondroprogenitor cells decreases bone density and increases marrow fat. *PLoS One* 5 (7), e11492.
- Refaey, M.E., McGee-Lawrence, M.E., Fulzele, S., Kennedy, E.J., Bollag, W.B., Elsalanty, M., et al., 2017. Kynurenine, a tryptophan metabolite that accumulates with age, induces bone loss. *J. Bone Miner. Res.* 32 (11), 2182–2193.
- Reid, J.C., Tanasijevic, B., Golubeva, D., Boyd, A.L., Porras, D.P., Collins, T.J., et al., 2018. CXCL12/CXCR4 signaling enhances human PSC-derived hematopoietic progenitor function and overcomes early in vivo transplantation failure. *Stem Cell Reports* 10 (5), 1625–1641.
- Reyes Ocampo, J., Lugo Huitrón, R., González-Esquivel, D., Ugalde-Muñiz, P., Jiménez-Anguiano, A., Pineda, B., et al., 2014. Kynurenines with neuroactive and redox properties: relevance to aging and brain diseases. *Oxidative Med. Cell. Longev.* 2014, 1–22.
- Ripoll, C.B., Bunnell, B.A., 2009. Comparative characterization of mesenchymal stem cells from eGFP transgenic and non-transgenic mice. *BMC Cell Biol.* 10, 3.
- Rüegger, S., Großhans, H., 2012. MicroRNA turnover: when, how, and why. *Trends Biochem. Sci.* 37 (10), 436–446.
- Sanchez-Martin, L., Sanchez-Mateos, P., Cabanas, C., 2012. CXCR7 impact on CXCL12 biology and disease. *Trends Mol. Med.* 19 (1), 12–22.
- Sas, K., Szabo, E., Vecsei, L., 2018. Mitochondria, oxidative stress and the kynurenine system, with a focus on ageing and neuroprotection. *Molecules (Basel, Switzerland)* 23 (1).
- Schaffner, M.B., Cheung, W.-Y., Majeska, R., Kennedy, O., 2013. Osteocytes: master orchestrators of bone. *Calcif. Tissue Int.* 94 (1), 5–24.
- Schönherr, E., Haussler, H.-J., 2000. Extracellular matrix and cytokines: a functional unit. *Dev. Immunol.* 7 (2–4), 89–101.
- Shi, S., Kanasaki, K., Koya, D., 2016. Linagliptin but not Sitagliptin inhibited transforming growth factor-beta2-induced endothelial DPP-4 activity and the endothelial-mesenchymal transition. *Biochem. Biophys. Res. Commun.* 471 (1), 184–190.
- da Silva Meirelles, L., 2006. Mesenchymal stem cells reside in virtually all post-natal organs and tissues. *J. Cell Sci.* 119 (11), 2204–2213.
- Skog, J., Wurdinger, T., van Rijn, S., Meijer, D.H., Gainche, L., Sena-Esteves, M., et al., 2008. Glioblastoma microvesicles transport RNA and proteins that promote tumour growth and provide diagnostic biomarkers. *Nat. Cell Biol.* 10 (12), 1470–1476.
- Souza, L.C., Jesse, C.R., Del Fabbro, L., de Gomes, M.G., Gomes, N.S., Filho, C.B., et al., 2018. Aging exacerbates cognitive and anxiety alterations induced by an intracerebroventricular injection of amyloid-beta1-42 peptide in mice. *Mol. Cell. Neurosci.* 88, 93–106.
- Stenderup, K., 2003. Aging is associated with decreased maximal life span and accelerated senescence of bone marrow stromal cells. *Bone* 33 (6), 919–926.
- Suh, J.S., Lee, J.Y., Choi, Y.S., Chung, C.P., Park, Y.J., 2013a. Peptide-mediated intracellular delivery of miRNA-29b for osteogenic stem cell differentiation. *Biomaterials* 34 (17), 4347–4359.
- Suh, J.S., Lee, J.Y., Choi, Y.S., Chong, P.C., Park, Y.J., 2013b. Peptide-mediated intracellular delivery of miRNA-29b for osteogenic stem cell differentiation. *Biomaterials* 34 (17), 4347–4359.
- Trivedi, C.M., Luo, Y., Yin, Z., Zhang, M., Zhu, W., Wang, T., et al., 2007. Hdac2 regulates the cardiac hypertrophic response by modulating Gsk3 beta activity. *Nat. Med.* 13 (3), 324–331.
- Tzeng, Y.S., Chung, N.C., Chen, Y.R., Huang, H.Y., Chuang, W.P., Lai, D.M., 2018. Imbalanced osteogenesis and adipogenesis in mice deficient in the chemokine Cxcl12/Sdfl in the bone mesenchymal stem/progenitor cells. *J. Bone Miner. Res.* 33 (4), 679–690.
- Vacher, S., Castagnet, P., Chemlali, W., Lallemand, F., Meseure, D., Pocard, M., et al., 2018. High AHR expression in breast tumors correlates with expression of genes from several signaling pathways namely inflammation and endogenous tryptophan metabolism. *PLoS One* 13 (1), e0190619.
- Valadi, H., Ekstrom, K., Bossios, A., Sjostrand, M., Lee, J.J., Lotvall, J.O., 2007. Exosome-mediated transfer of mRNAs and microRNAs is a novel mechanism of genetic exchange between cells. *Nat. Cell Biol.* 9 (6), 654–659.
- Vimalraj, S., Partridge, N.C., Selvamurugan, N., 2014. A positive role of microRNA-15b on regulation of osteoblast differentiation. *J. Cell. Physiol.* 229 (9), 1236–1244.
- Wang, K., Zhang, S., Weber, J., Baxter, D., Galas, D.J., 2010. Export of microRNAs and microRNA-protective protein by mammalian cells. *Nucleic Acids Res.* 38 (20), 7248–7259.
- Watson, J.D., Prokopec, S.D., Smith, A.B., Okey, A.B., Pohjanvirta, R., Boutros, P.C., 2017. 2,3,7,8 Tetrachlorodibenzo-p-dioxin-induced RNA abundance changes identify Akr3, Col18a1, Cyb5a and Glud1 as candidate mediators of toxicity. *Arch. Toxicol.* 91 (1), 325–338.
- William, D., Hill, S.H., 2016. Sudharsan Periyasamy-Thandavan Inventor Compositions and Methods for Treating Musculoskeletal Diseases and Disorders. US.
- Xiang, Z., Li, J., Song, S., Wang, J., Cai, W., Hu, W., et al., 2019. A positive feedback between IDO1 metabolite and COL12A1 via MAPK pathway to promote gastric cancer metastasis. *J. Exp. Clin. Cancer Res.* 38 (1), 314.
- Yamamoto, T., Hatabayashi, K., Arita, M., Yajima, N., Takenaka, C., Suzuki, T., et al., 2019. Kynurenine signaling through the aryl hydrocarbon receptor maintains the undifferentiated state of human embryonic stem cells. *Sci. Signal.* 12 (587), eaaw3306.
- Yang, F., Xue, F., Guan, J., Zhang, Z., Yin, J., Kang, Q., 2018a. Stromal-cell-derived factor (SDF) 1-alpha overexpression promotes bone regeneration by osteogenesis and angiogenesis in osteonecrosis of the femoral head. *Cell. Physiol. Biochem.* 46 (6), 2561–2575.
- Yang, S.-C., Wu, C.-H., Tu, Y.-K., Huang, S.-Y., Chou, P.-C., 2018b. Exposure to 2,3,7,8-tetrachlorodibenzo-p-dioxin increases the activation of aryl hydrocarbon receptor and is associated with the aggressiveness of osteosarcoma MG-63 osteoblast-like cells. *Oncol. Lett.* 16 (3), 3849–3857.
- Yu, L., Cecil, J., Peng, S.B., Schrementi, J., Kovacevic, S., Paul, D., et al., 2006. Identification and expression of novel isoforms of human stromal cell-derived factor 1. *Gene* 374, 174–179.
- Yun, C., Katchko, K.M., Schallmo, M.S., Jeong, S., Yun, J., Chen, C.H., et al., 2018. Aryl hydrocarbon receptor antagonists mitigate the effects of dioxin on critical cellular functions in differentiating human osteoblast-like cells. *Int. J. Mol. Sci.* 19 (1), 225.
- Zhang, W., Ou, G., Hamrick, M., Hill, W., Borke, J., Wenger, K., et al., 2008. Age-related changes in the osteogenic differentiation potential of mouse bone marrow stromal cells. *J. Bone Miner. Res.* 23 (7), 1118–1128.
- Zhang, Z., Qin, Y.W., Brewer, G., Jing, Q., 2012. MicroRNA degradation and turnover: regulating the regulators. *Wiley interdisciplinary reviews RNA* 3 (4), 593–600.